THE ROLE OF ACTIVATED THROMBIN-ACTIVABLE FIBRINOLYSIS INHIBITOR (TAFIA) IN ATHEROSCLEROSIS PROGRESSION

THE ROLE OF ACTIVATED THROMBIN-ACTIVABLE FIBRINOLYSIS INHIBITOR (TAFIA) IN ATHEROSCLEROSIS PROGRESSION

By DHULFIHA MUZAFAR GANI, B.H.Sc. (Hons)

A Thesis Submitted to the School of Graduate Studies in Partial Fulfilment of the Requirements for the Degree Master of Science

McMaster University

Master of Science (2018) McMaster University

(Department of Medical Sciences) Hamilton, Ontario

TITLE:	The role of activated thrombin-activable fibrinolysis inhibitor (TAFIa) in atherosclerosis progression
AUTHOR:	Dhulfiha Muzafar Gani B.H.Sc. (Honours) Health Sciences (University of Ottawa)
SUPERVISOR:	Dr. Paul Y. Kim, Ph.D.
NUMBER OF PAGES:	xiii, 70

Lay Abstract

Atherosclerosis is an inflammatory disease of large blood vessels that leads to unwanted clot formation on these weakened/compromised vessel walls. Eventually, the blood flow is hindered by these clots and the supply of oxygen and nutrients to vital organs are disrupted, leading to irreparable damage and death of these organs. As such, it, is the primary cause of heart attacks and strokes depending on the location of vessel occlusion. Thrombin activable fibrinolysis inhibitor (TAFI), when activated to TAFIa, contains both anti-inflammatory and antifibrinolytic properties. Therefore, it is likely that TAFI(a) would be involved in atherosclerosis development and/or progression, especially since other fibrinolytic factors have shown to be involved. Despite promising preliminary data, we found that TAFI(a) alone may minimally be involved in the overall atherosclerosis progression and development using a mouse model of atherosclerosis. We further investigate whether TAFI(a) can be used as a biomarker for early diagnosis of atherosclerosis.

Abstract

Atherosclerosis is a chronic inflammatory condition of larger arteries characterized by build-up of plaques in the vessel wall. Disruption of plaques results in superimposed thrombus formation, or atherothrombosis, leading to the occlusion of the blood vessels. Atherosclerosis is the primary cause of heart attacks and strokes. Recent studies show that various fibrinolytic factors influence atherosclerosis progression. A healthy fibrinolytic system is fundamental to mitigating the worsening of the lesion and atherosclerosis progression by rapidly removing unwanted microthrombi that is otherwise incorporated into the plaque. In this regard, the activated thrombin-activable fibrinolysis inhibitor (TAFIa), a potent antifibrinolytic metallocarboxypeptidase that attenuates clot dissolution, could influence atherosclerosis progression. Aside from its antifibrinolytic property, TAFIa also affects inflammation by inactivating anaphylatoxins and kinins. Therefore, TAFIa possesses the potential to influence atherosclerosis via antifibrinolytic and anti-inflammatory facets. We utilized mice deficient in apolipoprotein E ($ApoE^{-/-}$) as a model of atherosclerosis. Characterization of murine TAFIa determined that the functional half-lives at 37 and 25 ˚C were about 4.0 and 12.7 minutes, respectively. TAFIa was stable indefinitely at 0 ˚C. *In vitro* clot lysis assays were performed on the plasmas of C57BL/6J (wild-type) and $ApoE^{-/-}$ mice, aged 5, 10, 15 and 30+ weeks. No differences in clot lysis times were observed between the two genotypic classifications. TAFIa was directly quantified using our in-house assay, which showed decreased TAFIa levels in the $ApoE^{-/-}$ mice. Closer examination revealed that the plasma from the $ApoE^{-/-}$ mice was negatively influencing the TAFIa assay. Total TAFI zymogen levels in these samples appeared to

increase with age. Other biomarkers of inflammation were quantified using ELISAs; however, only IL-10 levels were measurable with slight elevation in the ApoE$^{-/-}$ mice across age, while IL-1β, TNF-α, and IL-6 was unquantifiable. Overall, TAFIa does not appear to influence atherosclerosis progression in ApoE$^{-/-}$ mice.

Acknowledgements

I would like to sincerely thank my supervisor Dr. Paul Kim for his invaluable guidance and support throughout my graduate study. His expertise in the field and passion for science has driven this project. Dr. Kim has always encouraged me to think critically and independently. His way of teaching and approach to science has promoted my ability to think as a scientist. I would also like to thank my committee members Dr. Peter Gross and Dr. Geoff Werstuck for their direction and contribution towards the completion of the study.

Special thanks to Shana Aadl Shaya for her time and effort into my microsurgery training. I am very grateful for her support and advice every step of the way, especially during stressful times.

I would like to thank my family for their unconditional support. This would not have been possible without them.

Lastly, I would like to thank my husband Ashik for his encouragement and patience throughout graduate school.

Table of Contents

List of Figures:

List of Tables:

List of Abbreviations

5IAF	5-iodoacetamidofluorescein
5IAF-Plg	plasminogen labeled with 5IAF
AAFR	N-(4-Methoxyphenylazoformyl)-Arg-OH · HCl
ApoA	apolipoprotein A
ApoE	apolipoprotein E
C_9-QSY	C_9-QSY-Maleiamide
CAD	coronary artery disease
CPN	carboxypeptidase N
FDPs	fibrin degradation products
Fg	fibrinogen
FPR-ck	Phe-Pro-Arg-chloromethylketone
FRET	fluorescence resonance energy transfer
iAP	$ApoE^{-/-}$ mice plasma that is depleted of functional TAFIa by incubating at 37° C for 30 minutes
IL-10	interleukin-10
IL-1β	interleukin-1 beta
IL-6	interleukin-6
LDL	low density lipoprotein
LDL-R	low density lipoprotein receptor
LT	lysis time
mTDP	mouse TAFI-deficient plasma
NHP	normal pooled human plasma
NMP	normal pooled mouse plasma
PAI-1	plasminogen activator inhibitor-1

Plg	plasminogen
Pn	plasmin
PPP	platelet-poor plasma
PRP	platelet-rich plasma
PTCI	potato tuber carboxypeptidase inhibitor
QSY-FDPs	C_9-QSY-labeled fibrin degradation products
RFU	relative fluorescence unit
SR-B1	scavenger receptor-1
TAFI	thrombin-activable fibrinolysis inhibitor
TAFIa	activated thrombin-activable fibrinolysis inhibitor
ΔLT	Difference in LT with and without PTCI inhibitor
TDP	TAFI-depleted plasma
TNK-tPA	tenectaplase; tissue-type plasminogen activator derivative with mutations T103N and N117Q in the kringle 1 domain, and A296K, A297H, A298R, A299R in the protease domain
tPA	tissue-type plasminogen activator
uPA	urokinase-type plasminogen activator
VFK-ck	Val-Phe-Lys-chloromethylketone
VLDL	very low density lipoprotein
WT	wild-type

Declaration of Academic Achievements

Dhulfiha Muzafar Gani contributed to conception and design of studies, obtained scholarship to support the studies, performed all experiments, analyzed and interpreted the data, and performed statistical analyses.

Dr. Paul Y. Kim contributed to conception and design of studies, obtained funding to support the studies, and critically reviewed and obtained results.

I. Introduction

1.1 Atherosclerosis

1.1.1 Etiology/mechanism

Atherosclerosis has been described as a well-known primary cause of heart attack and stroke (Lusis, 2000). Heart attacks and strokes are leading causes of mortality among Canadians. In 2012, heart disease and stroke accounted for 25% of all deaths in Canada (Statistics Canada, 2016a), representing a healthcare expenditure of about $21 billion each year (Statistics Canada, 2016b).

Atherosclerosis is a progressive inflammatory condition of large arteries characterized by the buildup of lipids and fibrous elements (Figure 1) (Lammeren et al., 2011; Lusis, 2000). According to the widely accepted "response-to-injury" model (Furie & Mitchell, 2012), the disease begins with an increased permeability of arterial endothelium to low density lipoprotein particles (LDL). This typically occurs in areas with high fluid shear stress such as sites of arterial bifurcations or curvatures where blood flow is disturbed (Lusis, 2000). The LDLs cross the endothelium and get deposited in the intima layer of the vessel. Deposited LDLs get oxidized and trigger an inflammatory response through stimulating the overlying endothelial cells to express pro-inflammatory adhesion molecules such as vascular cell adhesion molecule 1 (VCAM-1) and selectins (Cybulsky et al., 2001). The adhesion molecules attract monocytes and lymphocytes to the lesion and assist in their infiltration into the intima. In the intima, monocytes differentiate to macrophages and engulf the oxidized LDLs to become foam cells. These foam cells form the fatty streak that is typically observed in atherosclerosis. The foam

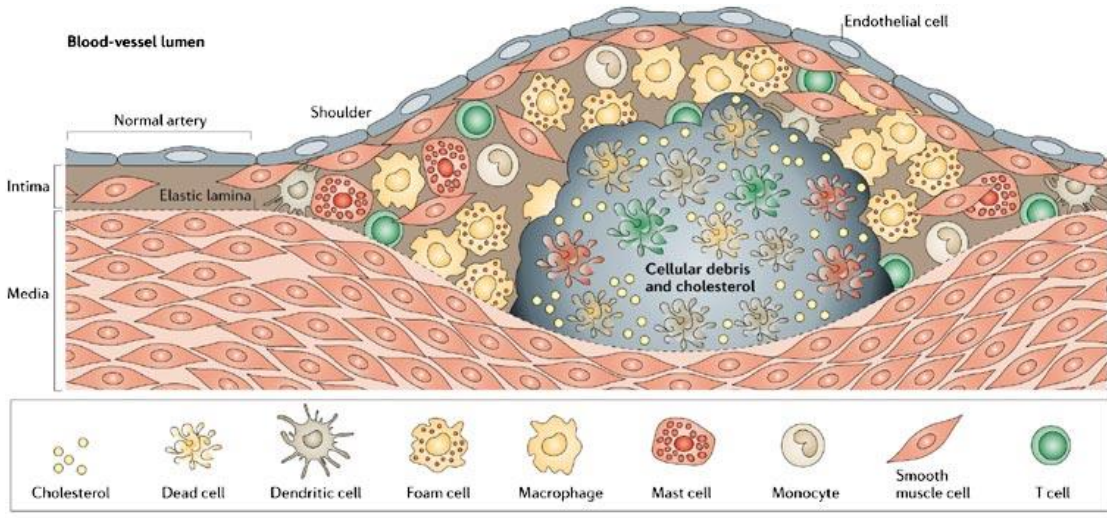

Figure 1. Atherosclerosis. An illustration of arterial atherosclerotic plaque in an inflammatory state through the recruitment of monocytes and leukocytes into the intima. Monocytes differentiate to macrophages and engulf oxidized LDLs to form foam cells, leading to further amplification of the immune response and migration of smooth muscle cells to form a fibrous cap over the atherosclerotic plaque. Dead foam cells release lipids and debris into their environment leading to the formation of a necrotic core. Diagram used from Hansson GK & Libby P., The immune response in atherosclerosis: a double-edged sword (Nat Rev Immunol (2006) 6(7):509) without permission.

cells further amplify the immune response by attracting more monocytes to the region and promoting the migration of smooth muscle cells from the medial layer to the intimal layer, allowing the formation of a fibrous cap over the atherosclerotic plaque (Lammeren et al., 2011; Lusis, 2000).

Foam cells eventually undergo apoptosis and release their contents including debris, pro-inflammatory mediators and oxidized lipids into their environment, which when combined with ineffective efferocytosis (Tabas, 2009; Van Vre, Ait-Oufella, Tedgui, & Mallat, 2012), lead to the development of a necrotic core (Ley, Miller, & Hedrick, 2011). A growing necrotic core, along with thinning of fibrous cap and stress from hemodynamic forces (Tegos, Kalodiki, Sabetai, & Nicolaides, 2001), heightens the risk of plaque destabilization making it vulnerable to ruptures (Ley et al., 2011). Ruptured plaque leads to atherothrombosis, or formation of blood clots superimposed on atherosclerotic plaques, as the rupture exposes a procoagulant surface. Throughout the lesion progression, fibrinogen is cleaved to fibrin on the luminal surface of the vessel, which results in multiple microthrombi formation. These thrombi later get incorporated into the mass of the plaque, thereby transforming into a fibrous tissue and increasing the size of the plaque (Tegos et al., 2001; Duguid, 1946).

Development of atherothrombosis and prolonged occlusion of blood flow in the arteries supplying blood to the brain or the heart can translate into ischemic stroke or heart attack, respectively, causing irreparable damage to these vital organs (Lammeren et al., 2011). Furthermore, the atherothrombotic clots in the aorta could embolize and lead to acute ischemic stroke. Therefore, identifying the mechanism(s) responsible for the

development and progression of atherosclerosis is important for developing new treatment strategies as current treatment options such as the use of statins, ACE inhibitors, anti-platelet medications, and beta-blockers, simply delay the onset of the disease (Acharji, Lakshmanadoss, Rudzinski, Stapleton, & Kaluski, 2013).

1.1.2 Biomarkers of atherosclerosis

Atherosclerosis has been viewed as a chronic vascular inflammation due to inflammatory responses prompted by endothelial injury, leading to LDL infiltration and leukocyte recruitment (Soeki & Sata, 2016). The leukocytes at the lesion enhance inflammation through the production of a variety of inflammatory cytokines and chemokines. Some of the important markers of inflammation include interleukin-1 beta (IL-1β), tumor necrosis factor-alpha (TNF-α), interleukin-6 (IL-6) and interleukin-10 (IL-10).

IL-1β, implicated in a range of cellular activities including cell proliferation, differentiation, and apoptosis, is an important mediator of the inflammatory response (Libby, 2017). It is also associated with a number of cardiovascular diseases (Libby, 2017). TNF-α is involved in a variety of signaling events, leading to necrosis or apoptosis in a cell (Idriss & Naismith, 2000). A high plasma concentration of TNF-α is associated with a high prevalence of atherosclerosis (Bruunsgaard, Skinhoj, Pedersen, Schroll, & Pedersen, 2000). IL-6 is also involved in acute phase inflammatory response, hematopoiesis, and immune responses (Tanaka, Narazaki, & Kishimoto, 2014). IL-6 has been shown to be significantly increased in patients with myocardial disease, ischemic cardiac disease,

stroke, and heart failure (Ridker, Rifai, Stampfer, & Hennekens, 2000; Cesari et al., 2003). In contrast, IL-10 is an anti-inflammatory cytokine that limits the production of several cytokines and chemokines including IL-1β, TNF-α and IL-6 (Couper, Blount, & Riley, 2008). In human atherosclerosis, IL-10 expression is associated with decreased signs of inflammation (Mallat et al., 1999).

Several studies have investigated the correlation and predictive power of these inflammatory biomarkers for the risk of an individual developing atherosclerosis (Thakore et al., 2007; Elkind et al., 2002; Corrado et al., 2010; Jenny et al., 2010). Although these markers are sensitive indicators of inflammation, they are not specific for detecting atherosclerosis (Germolec, Shipkowski, Frawley, & Evans, 2018). These indicators are common to most inflammatory diseases like allergy, asthma, cancer and other autoimmune diseases (Germolec et al., 2018).

Also, cytokine levels vary greatly among individuals and their expression is influenced by activating signals, its cellular targets, and physiological factors such as body fitness, feeding state, and acute stress (Zhou, Fragala, McElhaney, & Kuchel, 2010). Thus, normal cytokine levels differ between studies and are specific to their study population (Zhou et al., 2010).

Similarly, C reactive protein tests have been widely used in clinical practice to predict thrombotic incidents. These tests, however, are also not specific for atherosclerosis (Lammeren et al., 2011; Ammirati, Moroni, Norata, Magnoni, & Camici, 2015). Hong *et al.* found no significant association between subclinical atherosclerosis, defined as asymptomatic early stages of atherosclerosis (Kaczmarek, Lee, & McDonagh, 1993), and

a panel of ten inflammatory biomarkers including high-sensitivity C reactive protein, fibrinogen, intercellular adhesion molecule-1, interleukin-6, interleukin-18, lipoprotein-associated phospholipase-A2 activity and mass, monocyte chemoattractant protein-1, P-selectin, and tumor necrosis factor receptor-2 (Hong et al., 2013).

Chemokine (C-C motif) ligand 23 (CCL23), a potent chemoattractant for monocytes, and growth/differentiation factor (GDF-15), a stress response cytokine, are implicated in atherosclerosis progression (Castillo et al., 2010; Gopal et al., 2014). However, further investigation is required to warrant CCL23 and GDF-15 as reliable biomarkers.

Plasma oxidized-LDL level is elevated in coronary artery disease (CAD) patients and is considered as a potential biomarker of femoral atherosclerotic plaque, but not carotid atherosclerosis (Verhoye & Langlois, 2009). However, the association weakened after adjusting for other lipid parameters, and taking into account the biological and lifestyle variables affecting circulating oxidized-LDL levels (Verhoye et al., 2009).

1.1.3 Mice models of atherosclerosis

To investigate atherosclerosis and its development/progression in a mouse model, mice that are deficient in apolipoprotein E ($ApoE^{-/-}$) were developed (Zhang, Reddick, Piedrahita, & Maeda, 1992). ApoE is a ligand for lipoprotein receptors that mediate recognition of lipoproteins such as chylomicrons and very low-density lipoprotein (VLDL) and aid in its clearance. As a result, $ApoE^{-/-}$ mice have delayed and inefficient lipoprotein clearance leading to dyslipoproteinemia.

The ApoE$^{-/-}$ mice develop severe hypercholesterolemia and spontaneously develop atherosclerotic lesions, which can be accelerated upon introducing them to a high fat diet (Lo et al., 2016). The characteristics of these atherosclerotic lesions include fatty streaks to fibrous plaques, similar to those observed in humans. These ApoE$^{-/-}$ mice begin developing foam cell lesions between 8 to 10 weeks (Nakashima, Plump, Raines, Breslow, & Ross, 1994). The foam cell lesions progress to intermediate lesions around 15 weeks, and progress to fibrous plaque and advanced lesions at 20 weeks (Nakashima et al., 1994). The lesions are also spread out throughout the arterial tree (Nakashima et al., 1994).

LDLR$^{-/-}$ mice are also used as a model for atherosclerosis. Low density lipoprotein receptor (LDL-R) is a cell-surface receptor protein that is involved in the clearance of LDLs. These mice do not readily develop atherosclerosis on a regular chow-fed diet, thus, a high cholesterol diet with or without high fat is necessary to establish hyperlipidemia to prompt atherogenesis (Getz & Reardon, 2016). That being said, absence of LDL-R typically influences lipoprotein uptake and clearance, resulting in a larger prevalence of LDL as the cholesterol carrying lipoprotein in a regular chow-fed diet, whereas, cholesterol in ApoE$^{-/-}$ is predominantly carried on lipoprotein remnants rather than LDL (Getz & Reardon, 2012). The advantage of LDLR$^{-/-}$ mice is retained by the limited functions of LDL-R whereas, ApoE has functions affecting macrophage biology, immune function and adipose tissue biology, all of which may impact atherosclerosis development independent of plasma lipid levels (Getz et al., 2012). It is important to note that both ApoE$^{-/-}$ and LDLR$^{-/-}$ mice do not adequately reflect the lipid profiles found in type IIa hypercholesterolemia, characterized by elevated plasma LDL cholesterol levels, commonly observed in human

atherosclerosis (Iwaki, Sandoval-Cooper, Brechmann, Ploplis, & Castellino, 2006). The $LDLR^{-/-}$ mice do not have human-like elevation of LDLs due to their ability to convert apolipoprotein B (ApoB)-100 into ApoB-48 through ApoB editing catalytic peptide-1 (apobec1) (Hirano et al., 1996). The clearance of LDLs that contain that ApoB-48 variant does not depend on LDL-R, since ApoB-48 cannot bind to LDL-R. Mice with combined deficiencies of LDL-R and apobec1 ($L^{-/-}/A^{-/-}$) demonstrate high levels of LDL on normal diet and also have spontaneous atherosclerotic lesions in the aorta (Hirano et al., 1996).

In addition to these, mice lacking scavenger receptor B1 ($SR\text{-}B1^{-/-}$) mice crossed with $ApoE^{-/-}$ or $LDLR^{-/-}$ mice may be used as models of spontaneous or diet-induced coronary artery atherosclerosis. Scavenger receptor B1 (SR-B1) is a chief HDL metabolism regulator. This receptor aids cholesterol efflux from cells to HDL and mediates cholesteryl ester uptake from HDL in the liver (Trigatti & Fuller, 2016).

1.2 TAFI

1.2.1 Coagulation and fibrinolysis

The impact that an occlusive clot may have on the overall severity of a disease outcome is dependent on the dynamic balance between clot formation (thrombosis) and removal (fibrinolysis) (Okafor & Gorog, 2015). While the occlusion of major blood vessels by atherothrombosis leads to heart attacks and strokes, how the processes and components of thrombosis and fibrinolysis influence the development and/or progression of atherosclerosis as a whole remains poorly understood.

Coagulation begins with the activation of various coagulation factors that assemble

on a procoagulant surface (Kalafatis, Egan, van, V, Cawthern, & Mann, 1997). The cascade of coagulation steps ultimately leads to thrombin generation, which cleaves soluble fibrinogen (Fgn). Fgn is 340 kDa soluble plasma protein comprised of three pairs of polypeptide chains connected by 29 disulfide bonds (Weisel, 2005). Thrombin cleaves Fgn, generating fibrin (Fn) monomers that can then polymerize to form an insoluble fibrin mesh (Weisel, 2005).

The process of fibrinolysis is the breakdown of the insoluble Fn clot to generate soluble fibrin degradation products (FDPs). In circulation, this process is predominantly driven by plasmin (Pn), which is activated from its precursor plasminogen (Plg) by tissue-type plasminogen activator (tPA) (Figure 2) (Hoylaerts, Rijken, Lijnen, & Collen, 1982). Plg is a 92 kDa single chain glycoprotein, circulating in plasma at a concentration of ~2 µM (Castellino & Powell, 1981). The zymogen Plg is converted to its active form Pn, a serine protease, by a cleavage at the Arg561-Val562 peptide bond (Castellino et al., 1981). Similarly, urokinase-type plasminogen activator (uPA) is able to activate Plg, which is also found in circulation as well as in the extracellular matrix of various tissues (Hoyer-Hansen et al., 1992). Although slow, tPA is able to activate Plg on its own. The presence of Fn, however, enhances this reaction by 3-orders of magnitude (Figure 2) (Kaczmarek et al., 1993). Initial generation of Pn results in preliminary digestion of Fn fibres generating plasmin-modified fibrin. The consequence of partially digesting fibrin is the generation and exposure of new C-terminal lysine and arginine residues that provide

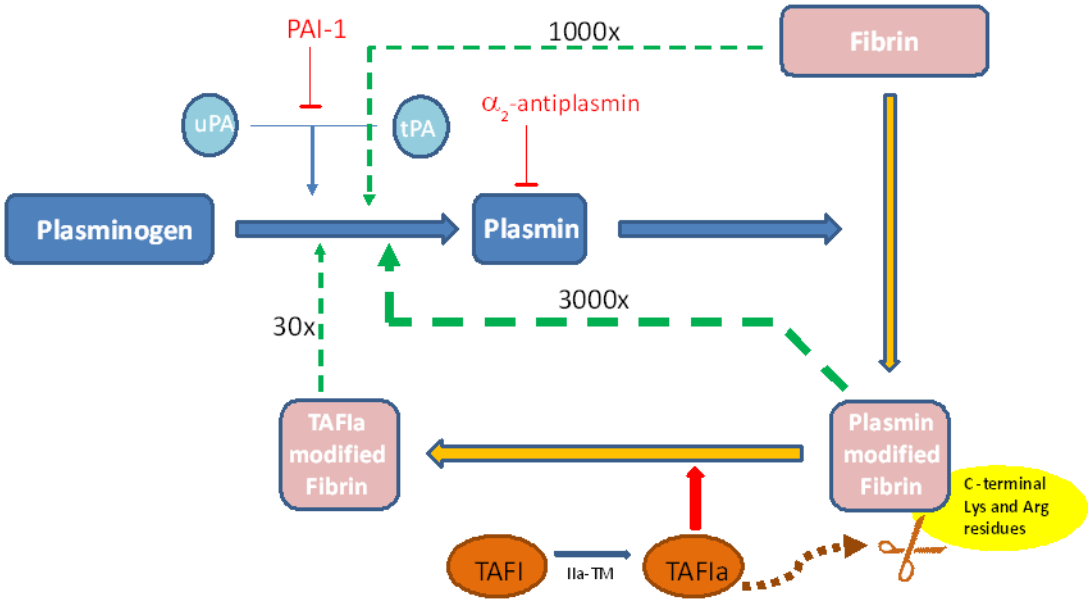

Figure 2. Fibrinolysis: Role of TAFIa in dampening fibrinolysis. The process of fibrinolysis involves plasminogen being activated to plasmin by its activators uPA and tPA in order to degrade fibrin. As plasmin begins cleaving fibrin to plasmin modified fibrin, it generates C terminal lysine residues that can bind tPA, plasminogen and plasmin. When this happens, the rate of plasminogen activation by tPA increases, resulting in the propagation of fibrinolysis. As a means to regulate fibrinolysis, along with other regulatory mechanisms involving PAI-1 and α_2-antiplasmin, TAFIa (formed when TAFI is activated by IIa-TM) clips the C-terminal lysine residues on plasmin modified fibrin converting it into TAFIa modified fibrin. TAFIa modified fibrin is unable to bind tPA and plasminogen, which makes it a poor cofactor for plasminogen activation resulting in fibrinolysis attenuation. uPA – urokinase plasminogen activator; tPA – tissue-type plasminogen activator; PAI-1 – plasminogen activator inhibitor-1; TAFI – thrombin activable fibrinolysis inhibitor, IIa – thrombin; TM – thrombomodulin.

additional binding sites for both Plg and tPA. The presence of additional Plg/tPA binding sites in plasmin-modified fibrin results in further enhancement of Plg activation by tPA compared with intact Fn (Li et al., 2014). Unlike tPA, however, uPA does not exhibit Fn dependence as it lacks the necessary kringle domain to bind Fn (Lee et al., 1988).

As unregulated fibrinolysis could lead to bleeding diathesis, mechanisms are in place to inhibit or down-regulate fibrinolysis when it is no longer needed. Both tPA and uPA can be inhibited by plasminogen activator inhibitor-1 (PAI-1) to regulate their activity, resulting in their short half-lives (Yasar, Kuru, Toksoy, & Agirbasli, 2014; Chapin & Hajjar, 2015). Furthermore, Pn is rapidly inhibited by α_2-antiplasmin so that Pn is not circulating in its active state (Schneider, Brufatto, Neill, & Nesheim, 2004). Another mechanism by which these processes are regulated is by thrombin-activable fibrinolysis inhibitor (TAFI), a procarboxypeptidase that once activated to TAFIa attenuates clot lysis by down-regulating Plg activation and enhancing Pn inhibition (Walker & Nesheim, 2001).

1.2.2 TAFI

TAFI is a 56 kDa procarboxypeptidase that circulates in plasma at a concentration of ~73 nM, made up of 401 residues in length (Bajzar, Manuel, & Nesheim, 1995). It is encoded by the *CPB2* gene and is mainly secreted by the liver and megakaryocytes (Lin et al., 2011). The gene spans for about 48 kb and is found on chromosome 13q14.11 (Vanhoof et al., 1996). Two pools of TAFI has been identified to be present in blood. The plasma pool accounts for the majority of TAFI in blood, and the platelet pool consists of < 0.1% of blood TAFI (Mosnier, Buijtenhuijs, Marx, Meijers, & Bouma, 2003). TAFI from the

two pools are similar in their enzymatic properties and thermal instability. Their glycosylation pattern, however, is different suggesting that platelet TAFI is produced by megakaryocytes and not endocytosed from plasma (Mosnier et al., 2003; Schadinger, Lin, Garand, & Boffa, 2010).

TAFI consists of a catalytic domain and an activation peptide region. The N-terminal activation peptide region spans from Phe1 to Arg92. TAFI activation involves a single cleavage at Arg92, resulting in the release of the activation peptide (Eaton, Malloy, Tsai, Henzel, & Drayna, 1991). This makes the active site readily accessible to its substrates. TAFIa is categorized as a metallo-carboxypeptidase due to the presence of a zinc ion in its active site core, which is essential in catalyzing the hydrolysis of the peptide bond in its substrates (Plug & Meijers, 2016).

TAFIa attenuates fibrinolysis by removing the newly exposed C-terminal lysine and arginine residues on plasmin-modified fibrin and converting it to TAFIa-modified fibrin (Walker et al., 2001). There are several consequences as a result of this process: 1) the number of Plg and tPA binding sites are reduced, which ultimately reduces Pn formation (Walker et al., 2001), 2) the protection of Pn from inhibition by α_2-antiplasmin afforded by binding to Fn is reduced (Schneider & Nesheim, 2004), and 3) reduced Pn formation and availability results in dampened Pn-dependent conversion of intact Plg (Glu-Plg) to a variant that is a better substrate for tPA/uPA by 20-fold (Lys-Plg) (Horrevoets, Pannekoek, & Nesheim, 1997). Therefore, TAFIa is a major regulator of fibrinolysis.

There are no known endogenous TAFIa inhibitors. Inhibition is thought to be its intrinsic thermal instability that leads to spontaneous inactivation (Schneider et al., 2002).

Interestingly, the functional half-lives of the two TAFIa variants due to naturally occurring polymorphisms at position 325 differ greatly; the Ile variant displays a half-life almost 2-fold greater than the more predominant Thr variant (Schneider et al., 2002). Additionally, because TAFIa inactivation is due to its thermal instability, the half-lives are sensitive to temperature: the half-lives at 37 ℃ are 8 minutes and 15 minutes, while at 22 ℃ are 77 minutes and 147 minutes for the Thr and Ile variants, respectively (Declerck, 2011). At 0 ℃ or below, however, TAFIa is thought to be indefinitely stable. The other two naturally occurring variants with alanine or threonine at position 147 do not affect its thermal stability.

1.2.3 The role of TAFIa in inflammation

In addition to its role in Fn clot protection, TAFIa also acts as an anti-inflammatory molecule at local sites of tissue injury (Leung, Nishimura, & Myles, 2008). It acts as a regulator of inflammation through inactivating kinins and anaphylatoxins. TAFIa cleaves bradykinin, C3a, C5a, and thrombin-cleaved osteopontin (Shinohara et al., 1994; Campbell, Lazoura, Okada, & Okada, 2002; Myles et al., 2003a). Hydrolysis of these substrates by TAFIa is as efficient as that of plasmin-modified fibrin. Osteopontin is involved in cell-cell and cell-matrix interactions, important in inflammation. It is also present in the subendothelial matrix of vessels involved in atherosclerosis (Myles et al., 2003b). Inactivation of C5a results in the inhibition of its neutrophil recruitment. Since atherosclerosis is characterized by chronic inflammation and TAFIa has known anti-inflammatory function, it is feasible that the role of TAFIa in inflammation may provide a

link between fibrinolysis and atherosclerosis development and/or progression.

1.2.4 TAFI/TAFIa: Correlations and associations with diseases

High levels of TAFI are correlated with increased risks for diseases like stable angina pectoris, coronary artery disease, myocardial infarction, and venous thrombosis (Fernandes et al., 2015; Santamaria et al., 2004; Zorio et al., 2003; van Tilburg, Rosendaal, & Bertina, 2000). While investigating the role of TAFI in various diseases certainly has merit, it is equally, if not more, important to investigate the role and quantify circulating levels of TAFIa that is present in these patients. This is especially significant as TAFIa is transient with a short half-life. This allows for TAFIa to potentially serve as a biomarker for various disease states.

Few studies report a relationship between high TAFIa concentration and circulatory diseases. Leebeek *et al.* tested the difference in functional TAFIa levels between people who had their first ischemic stroke and matched controls. The study found that subjects in the highest quartile of TAFIa levels had increased risk of ischemic stroke compared to the lowest quartile (Leebeek et al., 2005). Similarly, TAFIa levels were associated with increased risk of cardiovascular death (Tregouet et al., 2009). These studies provide more reasons to suspect that TAFIa plays a role in the progression of atherosclerosis leading to cardiovascular events.

TAFIa inhibitors are able to promote tPA-mediated fibrinolysis through increasing Pn generation and enhanced Pn protection from inhibition by α_2-antiplasmin. TAFIa inhibitors include potato tuber carboxypeptidase inhibitor (PTCI), a 39-amino acid protein

that competitively inhibits TAFIa (Ryan, Hass, & Kuhn, 1974), and 2-guanidinoethylmercaptosuccinic acid (GEMSA) (Fricker, Plummer, Jr., & Snyder, 1983). Interestingly, these small inhibitor molecules exert a biphasic dose-dependent characteristic of TAFIa activity. At high concentrations, both inhibitors increase tPA-dependent fibrinolysis *in vitro* while at low concentrations, they stabilize the TAFIa molecule, thus increasing its apparent half-life and increase the potency of TAFIa for inhibiting fibrinolysis (Schneider & Nesheim, 2003). In a rabbit thrombosis model, PTCI has been shown to promote fibrinolysis when administered in conjunction with tPA, without increased bleeding (Klement, Liao, & Bajzar, 1999). PTCI also significantly inhibited murine thrombosis in a model of ferric-chloride induced vena cava thrombosis (Wang, Smith, Hsu, Ogletree, & Schumacher, 2006), however, the effects were not significant when a severe $FeCl_3$-mediated thrombosis was inflicted. Aminopyridine mercaptane (AZD9684), a small molecule TAFIa inhibitor has been evaluated in a phase II study in patients with pulmonary embolism, however, the development of this drug was ceased due to its limited activity (Willemse, Heylen, Nesheim, & Hendriks, 2009; Zhou et al., 2017). Another small molecule, DS-1040, has overcome the problem of low activity and exhibit dose-dependent TAFIa inhibition when administered to healthy volunteers (Zhou et al., 2017). The drug is currently in phase II trials, administered to patients with submassive pulmonary embolism and ischemic stroke patients ineligible for tPA-thrombolysis (Henderson, Weitz, & Kim, 2018).

1.3 Fibrinolysis and atherosclerosis

A healthy fibrinolytic system is able to prevent vessel occlusion without bleeding complications. This raises a potential link between fibrinolysis defect and the progression of atherosclerosis as evidenced by the cross-talk between fibrinolytic proteins such as Plg and Fgn, and atherosclerosis (Okafor et al., 2015; Xiao et al., 1997; Eitzman, Westrick, Xu, Tyson, & Ginsburg, 2000; Xiao et al., 1998; Bicakcigil, Tasan, Tasdelen, Mutlu, & Yavuz, 2011; Kremen et al., 2008). Deficiency of Plg has been linked with accelerated atherosclerotic intimal lesion progression (Xiao et al., 1997). Factors that affect the level of Plg activation also play a role. For instance, PAI-1 directly inhibits tPA and its absence could be expected to enhance fibrinolysis (Eitzman et al., 2000). Deficiency of PAI-1 has been identified to have a protective effect against the pathogenesis of atherosclerosis (Eitzman et al., 2000; Bicakcigil et al., 2011).

Similarly, TAFIa, as a key attenuator of fibrinolysis could play a role in plaque formation and/or stabilization. Therefore, we are interested in studying the role of TAFIa in the development and/or progression of atherosclerosis. The microenvironment of the atherosclerotic lesions plays a vital role in impacting its stability. Fn-targeted paramagnetic nanoparticles were able to detect occult microthrombi within the intimal surface of atherosclerotic lesions (Flacke et al., 2001). Lesions with increased Fn deposition, or microthrombi, are identified to be the vulnerable plaques, ultimately leading to plaque destabilization (Flacke et al., 2001). By indirectly modulating Plg levels near the thrombi, TAFIa may influence atherosclerotic lesion progression. In addition, TAFIa may amplify the impact of atherothrombotic events by attenuating the removal of occluding thrombi.

Identification of the TAFIa-mediated link between fibrinolysis and atherosclerosis/atherothrombosis would be a novel finding that opens new avenues for developing new treatment and prevention options for atherosclerosis/atherothrombosis.

We will also evaluate in mice how TAFIa levels correlate with other well-established biomarkers of inflammation such as IL-1β, TNF-α, IL-6, and IL-10 to identify whether TAFIa levels can also serve as an indicator for inflammation and atherosclerosis.

1.4 Hypothesis and aims

Hypothesis: Functional TAFIa levels are positively correlated with atherosclerosis progression and is a biomarker for detection of atherosclerotic plaque development and/or progression.

Specific Aims:

1) Compare clot lysis times of plasma samples collected from 5, 10, 15 and 30+ weeks old ApoE$^{-/-}$ mice with age- and sex-matched C57BL/6J wild-type mice plasma samples.
2) Identify and quantify functional TAFIa levels in mice plasma samples using the in-house functional assay and a turbidity-based clot lysis assay, in the presence or absence of its inhibitor, PTCI.
3) Quantify levels of TAFI zymogen in all samples via ELISA.
4) Measure inflammatory biomarkers such as IL-1β, TNF-α, IL-6, and IL-10 in the ApoE$^{-/-}$ plasma samples and compare it to age- and sex-matched wild-type mice

plasma samples using ELISA.

II. Methods and materials

2.1 Materials

Thrombin was obtained from Enzyme Research Laboratories (South Bend, IN, USA). Tenectaplase-tPA (TNK-tPA) and Solulin (truncated soluble form of thrombomodulin consisting residues 4-490) were a generous gift from Dr. Weitz (Thrombosis and Atherosclerosis Research Institute (TaARI), McMaster University, Hamilton, Ontario). Potato tuber carboxypeptidase inhibitor (PTCI) was purchased from Sigma (St. Louis, Missouri, USA). TAFI-depleted plasma (TDP) was prepared by passing Normal Human Plasma (NHP) over a 3 mL mAbT12D11-Sepharose 4B column equilibrated in 0.02 M Hepes, 0.15 M NaCl, pH 7.4 (HBS) with depletion of TAFI confirmed by a clot lysis assay performed with generated TDP in the presence or absence of Solulin (50). Mouse TAFI-deficient plasma (mTDP) was prepared by pooling the plasmas obtained from 6 TAFI knock-out mice. C57BL/6J (5, 10, 15 and 30+ weeks old; male and female) and $ApoE^{-/-}$ (C57BL/6J background; 5, 10, 15 and 30+ weeks old; male and female) mice were a kind gift of Dr. Werstuck (Thrombosis and Atherosclerosis Research Institute (TaARI), McMaster University, Hamilton, Ontario). The mice were housed in micro-isolator cages on a constant 12h light/12h dark cycle with controlled temperature and humidity, and given access to food (regular chow) and water *ad libitum*. Normal mouse plasma (NMP) was prepared by combining the plasmas of 10 C57BL/6J wild-type (WT) mice. TAFI-TT (recombinant TAFI with threonine at position 147 and threonine at 325) was also isolated using a Sepharose 4B column of immobilized mouse anti-TAFI antibody (mAbT12D11, gifted by Dr. Ann Gils (Leuven, Belgium). Phe-Pro-

Arg-chloromethylketone (FPR-ck) and Val-Phe-Lys-chloromethylketone (VFK-ck) were obtained from EMD Millipore Corporation (Billerica, MA, USA). C_9-QSY maleiamide (QSY) and 5-iodoacetamidofluorescein (5IAF) were obtained from Molecular Probes (Eugene, OR, USA) and Marker Gene Technologies, Inc. (Eugene, OR, USA), respectively. QSY-labeled fibrin degradation products (QSY-FDP) was generated (Kim et al., 2008) by selectively reducing Fg by β-mercaptoethanol and subsequently labeling with QSY to generate QSY-Fg. QSY-Fg was then clotted and lysed with 5 nM thrombin, 2 nM calcium, and 40 nM plasmin. Clotting and lysis of the mixture was turbidimetrically monitored using a SpectraMax M2 microplate reader (Molecular Devices, CA). When the peak absorbance was reduced by 80%, lysis was stopped by the addition of 5 µM FPR-ck and 5 µM VFK-ck. A standard curve of TAFIa (0 to 200 pM final concentrations) was generated using our in-house TAFIa assay (Section 4.5) to verify the functionality of the obtained QSY-FDPs. Recombinant plasminogen labeled with 5IAF (5IAF-Plg) was prepared as described previously (Kim et al., 2008), using a Plg variant with its latent active site serine mutated to cysteine at position 741 (S741C) that was subsequently labeled with 5-IAF. Synthetic carboxypeptidase substrate N-(4-Methoxyphenylazoformyl)-Arg-OH HCl (AAFR) was purchased from Bachem Biosciences Inc., (Torrence, CA, USA). Quantikine ELISA kit for mouse IL-10 was purchased from R&D systems (Minneapolis, MN, USA). 4-plex Mouse Magnetic Luminex Assay was obtained from Bio-Techne (Minneapolis, MN, USA). ELISA kit that is specific for measuring mouse TAFI zymogen levels (mAb RT36A3F5, mAb RT30D8G6-HRP, and murine TAFI standards) was a generous gift from Dr. Paul Declerck (Katholieke Universiteit, Leuven, Belgium).

2.2 Blood collection using carotid cannulation and plasma isolation

Blood was collected from mice using carotid cannulation as described previously (Ni, Peleg, & Gross, 2012) with slight modifications (Figure 3). Briefly, the mice were anesthetized throughout the procedure using 3% isofluorane. Once the mouse was subdued, an incision was made and the right carotid artery isolated (Figure 3A). An artery clip was then used to stop the blood flow on the proximal end and a suture was used to tie the distal end (Figure 3B). The ends of the distal suture were taped together, pulled back and secured into position. This extended and elevated the position of the carotid artery. A small incision was then made towards the distal suture and a PE 10 (0.28 mm diameter) cannula that is connected to 1 mL 28 gauge-syringe, containing 80 µL of 4% citrate solution, was slowly inserted through this incision into the artery (Figure 3C). A tight second suture thread knot was then placed over the artery enveloping the cannula to immobilize the cannula. Once secured, the artery clip was released and the blood was drawn into the syringe at a steady speed. The collected blood was then transferred to an Eppendorf tube and stored on ice immediately. This is important for the purposes of measuring TAFIa levels in these blood samples due to the intrinsic thermal instability of TAFIa and its accompanying short half-life (Schneider et al., 2002). Furthermore, when the blood samples are collected for the purposes of measuring TAFIa levels, we added additional serine protease inhibitors Phe-Pro-Arg-chloromethylketone (FPR-ck) and Val-Phe-Lys- chloromethylketone (VFK-ck) to inhibit thrombin/tPA and plasmin activity,

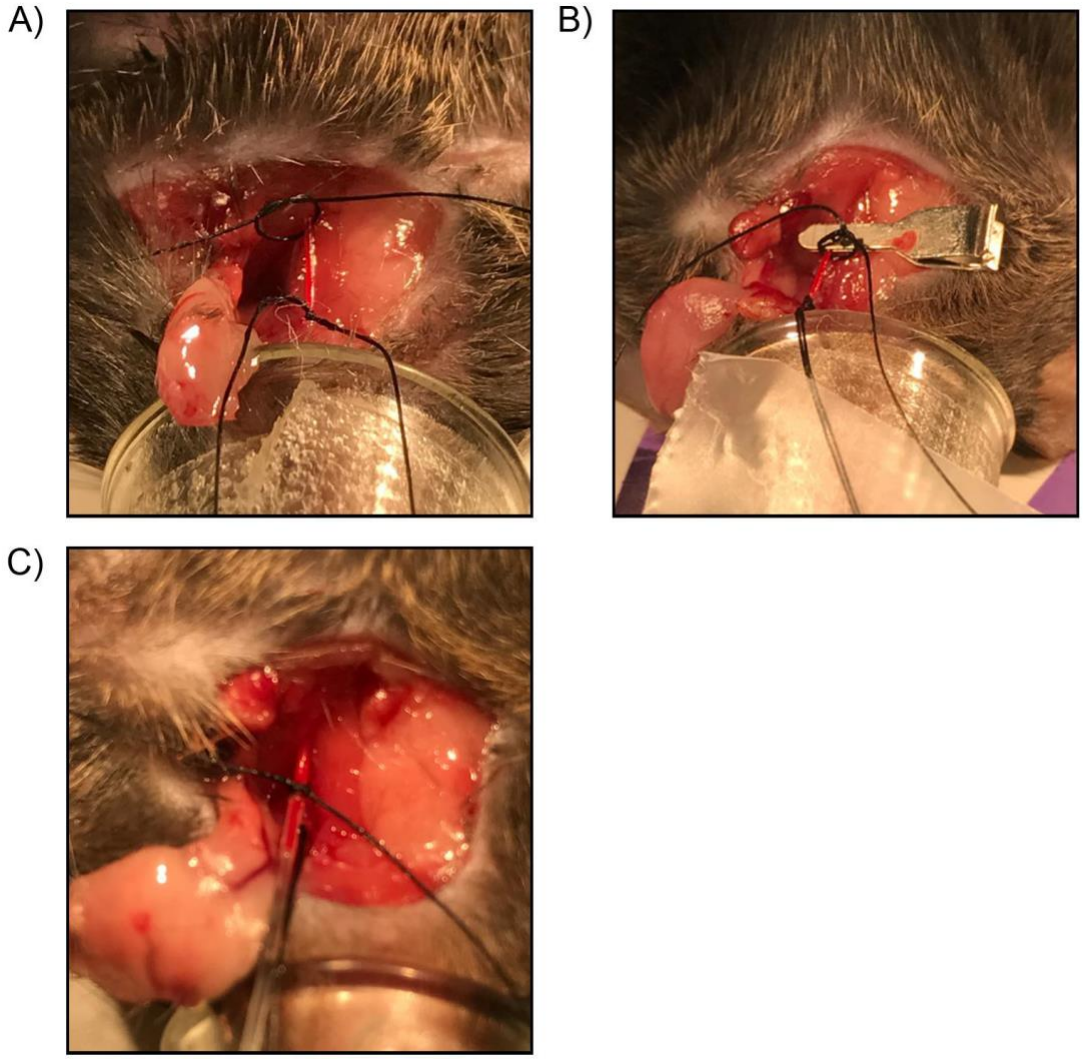

Figure 3. Cannulation of the carotid artery in collecting blood. A) Isolation and positioning of carotid artery: tied distal suture prevents the back-flow of blood and secures the carotid in place, while loose suture knot prepared to secure the incoming cannula in place, within the vessel. **B)** Introduction of artery clip to stop blood flow, permitting a clean area for the incision to be made. **C)** Cannula inside the artery, held and secured in place by suture thread knot. Artery clip is then released to allow the blood to flow into the cannula.

respectively (Foley, Kim, Mutch, & Gils, 2013).

From the collected blood, plasma is isolated immediately via two centrifugation steps as described previously (Dhurat & Sukesh, 2014) with slight modifications (Figure 4). Briefly, 800 µL of citrated blood was divided equally into two tubes, to which 200 µL of pre-chilled PIPES buffer (2.5 mM Pipes, 137 mM NaCl, 4 mM KCl, 0.1% Glucose, pH 7.4) is added and mixed. The addition of PIPES buffer increased the total plasma yield for each sample. Initially, samples were centrifuged at 200 × g for 20 min at 4°C to isolate the supernatant, which is the diluted platelet-rich plasma (PRP) without red blood cells (RBCs) and white blood cells (WBCs). The PRP was then transferred to a new tube and subjected to subsequent centrifugation at 3000 × g for 20 min at 4°C to remove platelets The supernatant, which contains the platelet-poor plasma (PPP) was then isolated, placed on ice and either used immediately or aliquoted to be snap frozen and stored at -80˚C.

2.3 Murine TAFIa characterization

While human TAFIa has been well characterized in the literature, murine TAFIa has not been extensively studied. The half-life of mouse TAFIa at 37˚C is reported to be 2-3 minutes [56]. However, the half-lives at 25˚C and 0˚C are unknown. To confirm and determine the half–lives of mouse TAFIa at these temperatures, TAFI in 900 µL of NMP was activated with thrombin (25 nM), $CaCl_2$ (5 mM), and Solulin (100 nM). After incubation at room temperature for 20 minutes, FPR-ck (1 µM) and VFK-ck (1 µM) were added to stop the reaction and vortexed to dislodge the clot. The clot was then centrifuged

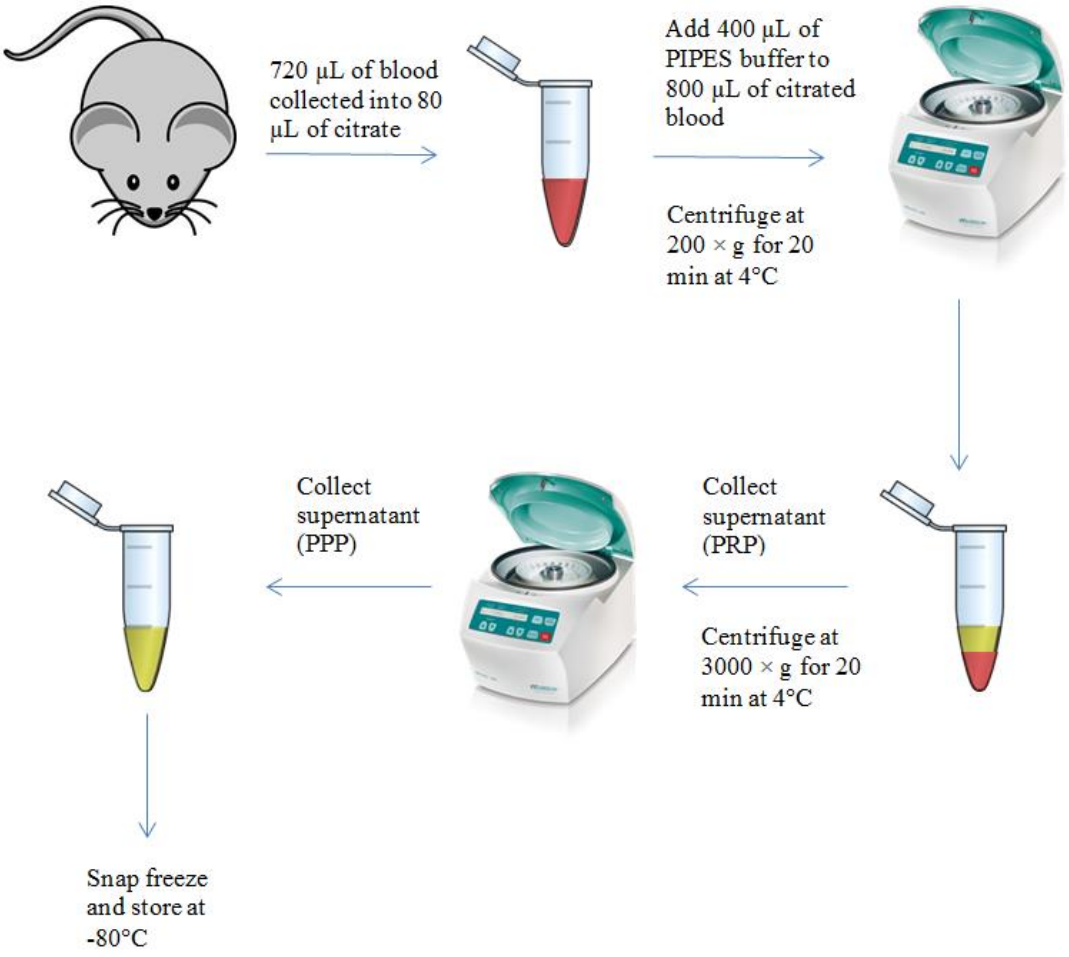

Figure 4. Centrifugation of blood to obtain platelet poor plasma (PPP) for clot lysis assays. Blood is obtained via carotid cannulation and plasma is isolated by centrifugation and storage at 4°C. Final plasma sample is then snap frozen and stored at -80°C until use. PRP – platelet rich plasma; PPP – platelet poor plasma.

for 10 minutes at 14,000 × g at 4˚C, after which the supernatant serum was collected. The obtained serum was incubated at 0˚C, 25˚C, or 37˚C, from which 50 µL of serum was removed at various time points and added to 50 µL of AAFR (280 µM). The time points for 0˚C, 25˚C or 37˚C were as follows: 0, 1, 2, 3, 5 and 7.5 hours, 0 to 45 min at 5 min intervals, and 0, 2, 4, 6.5, 9, 14 and 19 min, respectively.

The reactions are then monitored by measuring the absorbance reading at 349 nm at 1 minute intervals at 25˚C using SpectraMax M2 microplate reader (Molecular Devices, CA). Background carboxypeptidase N (CPN) activity was measured by pre-incubating the NMP at 37˚C for 30 minutes, whereby 50 µL of TAFIa-free NMP was then added to AAFR. The initial rate observed with CPN was then subtracted from the initial rates observed at varying time points. The initial rate at each time (V_t) were divided by the initial rate at t = 0 minute (V_0). The relative residual rate (V_t/V_0) was then plotted with respect to time. The functional half-life of TAFIa was then determined by fitting the data to the first-order decay model.

The effect of freeze thaw-cycle on TAFIa was also determined by comparing fresh NMP with NMP that had been through 1 and 2 cycles of freezing and thawing. Briefly, 50 µL of fresh or freeze-thawed NMP was added to 50 µL of AAFR (280 µM) and the reactions were monitored by absorbance as described above. The initial rates of fresh/freeze-thaw cycle (V_{ft}) were divided by the initial rate of fresh NMP (V_f), to determine the fraction of original TAFIa remaining after each freeze-thaw cycle.

2.4 Clot lysis assay

2.4.1 Clot lysis in mouse plasma

To measure the clot lysis times of the mouse plasma, a turbidity-based clot lysis assay was used, as described previously (Miles, Castellino, & Gong, 2003). Initially, a 96-well microtiter plate was pretreated with HBS with 1% Tween-80, and rinsed thoroughly prior to use. Human thrombin (10 nM) is used to generate clots in mouse plasma. However, because human tPA is a poor activator of the mouse fibrinolytic system (Matsuo, Lijnen, Ueshima, Kojima, & Smyth, 2007), we used tenecteplase (TNK-tPA), a mutant variant of tPA with six key mutations. TNK-tPA involves tissue-type plasminogen activator derivative with mutations T103N and N117Q in the kringle 1 domain, and A296K, A297H, A298R, A299R in the protease domain (Thomas et al., 1994). Another modification made to optimize the assay was to conduct the clot lysis reactions at 25°C instead of 37°C. This is to compensate for the instability of murine TAFIa, which has a half-life ($t_{1/2}$ = 2.8 ± 0.2 minutes) that is shorter than humans ($t_{1/2}$ = 8 to 15 min) (Hillmayer, Ceresa, Vancraenenbroeck, Declerck, & Gils, 2008b). Assuming that the functional characteristics of mouse TAFIa is similar to that of human, (Marx et al., 2000), conducting reactions at 25°C would increase its half-life and may widen the window of separation between lysis times of plasmas, with or without elevated TAFIa levels.

2.4.1.1 TNK-tPA optimization

To identify the appropriate concentration of TNK-tPA to be used to achieve a desirable clot lysis time of around 30 minutes, clots were formed using thrombin (10 nM)

and lysis initiated with TNK-tPA at final concentrations ranging between 0 and 100 nM. In addition, to prevent premature clot formation, 2 µL of $CaCl_2$ (15 mM) is also placed separately into the well prior to freshly generated NMP addition (1:3 dilution) into the wells, to a final volume of 100 µL. The reactions are carried out at 25˚C and monitored with turbidity readings measured at 400 nm at 1 minute intervals. The lysis times are then taken as the time required to reach half-maximal turbidity change from the start of the reaction.

2.4.1.2 Lysis in mouse plasma using clot optimized TNK-tPA concentration

Once the optimal TNK-tPA concentration was identified, clot lysis attenuation in the mouse plasma system was investigated. To achieve this, 5 µL of TNK-tPA (optimized concentration), 5 µL of human thrombin (10 nM), and 2 µL of $CaCl_2$ (15 mM) was placed separately in the reaction well. The reaction was initiated with 49.5 µL of isolated plasma (comprised of 33 µL of mouse plasma and 16.5 µL PIPES buffer) and 38.5 µL HBS with 0.01% Tween-80 (HBST), resulting in a 1:3 dilution of plasma in a final reaction volume of 100 µL. The reactions were carried out at 25˚C and monitored with turbidity readings measured at 400 nm at 1 min intervals. The lysis times are quantified as described above. These lysis experiments are then repeated in the presence of a TAFIa inhibitor, potato tuber carboxypeptidase inhibitor (PTCI, 10 µM), to discern the role of TAFIa in the lysis times observed. The experiments were performed alongside a clot lysis reaction initiated with NMP, to serve as an internal control to correct for day-to-day variability.

2.4.2 TAFIa-mediated clot prolongation

The reactions with and without PTCI were conducted, in duplicates, simultaneously on the same microtiter plate. Lysis time of reaction with PTCI (duplicate 1) was subtracted from the lysis time of reaction without PTCI (duplicate 1) to obtain change in LT (ΔLT), which quantifies TAFIa-mediated time delay, in minutes. The ΔLT was also obtained from the second set of duplicates and the average of ΔLT from the duplicates was taken to be the mean ΔLT for the sample. The ΔLT of mice from each category was then averaged.

2.4.3 Turbidity comparisons of clot lysis profiles in mice plasma

To determine if there are any baseline turbidity differences in the plasma samples obtained and if there are variances in plasma clot structures, we compared two parameters such as the baseline turbidity and the change in turbidity during clot-lysis. The baseline turbidity (OD_{min}) is taken as the minimum turbidity/optical density reading (O.D.) following complete lysis. The change in O.D. (ΔOD) is calculated as the difference between OD_{min} and maximum O.D. during clot-lysis. The average OD_{min} and ΔOD for each group (stratified based on genotype, age and sex) were obtained.

2.5 Measurement of TAFIa levels in mouse plasma

To determine if TAFIa levels fluctuated with atherosclerosis and/or age, TAFIa was measured in all samples. To quantify TAFIa, plasma samples were isolated carefully to preserve maximal TAFIa function as described previously (Foley et al., 2013). The samples were then subjected to TAFIa measurements using a Fluorescence Resonance Energy

Transfer (FRET) based in-house assay (Kim et al., 2008) that specifically measures functional levels of TAFIa in plasma (Figure 5). Conversion of QSY-Fg to QSY-Fn by thrombin and subsequent digestion to QSY-FDPs by Pn results in the generation of newly exposed C-terminal lysine residues that binds 5IAF-Plg. When 5IAF-Plg binds QSY-FDPs, its fluorescence is quenched. Once TAFIa is introduced in the system, it cleaves these C-terminal lysine binding sites on QSY-FDPs, resulting in a shift of equilibrium towards the unbound state and increased fluorescence of 5IAF-Plg in a TAFIa-concentration dependent manner (Kim et al., 2008).

To measure TAFIa levels in plasma, a 96-well microtiter plate was pretreated with HBS with 1% Tween-80 and washed thoroughly. QSY-FDPs (1 µM) and 5IAF-Plg (0.1 µM) were combined and brought to 80 µL with the final NaCl concentration adjusted to 0.2 M. The baseline fluorescence of the mixture is monitored at excitation 480 nm and emission 520 nm, with a 495 emission cut-off filter using a SpectraMax M2 microplate reader (Molecular Devices, CA) (Kim et al., 2008). TAFIa standards are generated by activating TAFI-TT (1 µM) by adding thrombin (25 nM) in the presence of Solulin (100 nM) and $CaCl_2$ (5 mM) in HBST and made to appropriate concentrations using mTDP. Once the signal is stabilized, the reaction is initiated by the addition of 20 µL of plasma that contain either TAFIa standards in mTDP or samples) to the QSY-FDPs/5IAF-Plg mixture. The standard curve is generated by plotting the initial rate of

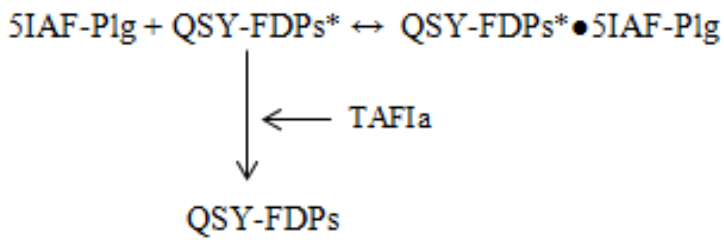

Figure 5. Interaction of 5IAF-Plg and QSY-FDPs in TAFIa assay. As 5IAF-Plg binds to C-terminal lysine residues (asterisk) on QSY-FDPs, its fluorescence is quenched. The bound and unbound forms of QSY-FDPs reach equilibrium. When TAFIa is introduced in the system, it cleaves the C-terminal lysine residues thereby dissociating 5IAF-Plg from QSY-FDPs. Dissociation results in fluorescence increase in 5IAF-Plg and the rate of increase is used to measure TAFIa. Adapted from: Kim PY, Foley J, Hsu G, Kim PY, Nesheim ME. An assay for measuring functional activated thrombin-activatable fibrinolysis inhibitor in plasma. *Anal Biochem* 2008; **372:** 32-40.

fluorescence increase with respect to known levels of TAFIa and the specific activity determined was then used to quantify TAFIa levels in mice samples.

In addition, to determine if plasma obtained from the $ApoE^{-/-}$ mice interfered with the TAFIa assay, TAFIa standard curves were also generated in parallel using either mTDP or plasma from the $ApoE^{-/-}$ mice that is depleted of functional TAFIa by incubating at 37° C for 30 minutes (iAP).

2.6 Measurement of TAFI zymogen levels in mouse plasma

To determine if TAFI zymogen levels varied with age/genotype, TAFI levels were quantified in the plasma samples using a sandwich-type ELISA that was generously provided by Dr. Paul Declerck (KU Leuven, Belgium) (Hillmayer et al., 2008a). Briefly, the capture antibody against TAFI (mAb RT-36A3F5) was diluted with PBS (0.04 M phosphate, 0.14 M NaCl, pH 7.4) and added to the wells of a polystyrene microtiter plate. After incubation for 48 hours at 4˚C, the wells were emptied and treated with PBS containing 10 g/l bovine serum albumin (BSA), after which the plate was washed and stored at -20˚C until use. The samples were then incubated in the coated wells for 18 hours at 4˚C, following which the conjugate antibody (mAb RT 30D8G6-HRP) was added. After two hours of incubation at room temperature, the wells were emptied, washed, and the substrate solution composed of 0.1 M citrate, 0.2 M sodium phosphate buffer pH 5.0, containing 300 µg/ml o-phenlylenediamine and 0.003% hydrogen peroxide was added. The substrate solution was allowed to react for one hour and the reaction was stopped using 4 M sulfuric acid. The absorbance of the resulting solution was then measured at 492 nm and

TAFI concentrations were determined using the specific activity determined experimentally.

2.7 Measurement of inflammatory biomarkers in mouse plasma

The Luminex multiplex assay was customized to measure three inflammatory biomarkers: IL-1β, TNF-α, and IL-6, simultaneously, using a Bio-Plex 200 Systems (Bio-Rad, Hercules, CA, USA). Mouse IL-10 levels were quantified using the Quantikine ELISA, which was performed according to manufacturer's instructions.

2.8 Statistical Analysis

Data analyses were performed using SPSS version 24.0 (IBM) and GraphPad Prism version 7.0. Normality of lysis times was assessed by the use of the Shapiro-Wilk test and Q-Q plots. For normally distributed data, we compared groups using the Independent t-test. As means of a non-parametric test, the Mann-Whitney U test was used to analyze medians of groups. A Jonckheere-Terpstra Test was applied to assess for trends across an ordinal variable (*i.e.* age). A Kendall's tau-b was calculated to identify the direction of the trend after the Jonckheere-Terpstra Test. Two-way ANOVA with post hoc Bonferroni correction was used to analyze the differences in TAFIa, TAFI, and IL-10 levels. P-value < 0.05 was used as an indicator of significance with most being 2-tailed tests (except for Jonckheere-Terpstra Test).

III. Results

3.1 Characterization of murine TAFIa

While the half-life of mouse TAFIa has been reported at 37°C (Hillmayer et al., 2008b), half-lives were determined using first order exponential decay equation (Figure 6). The half-lives of murine TAFIa are summarized in Table 1. Mouse TAFIa at 37°C was determined to have a half-life of 4.0 ± 0.4 minutes, which is slightly longer than the previously reported half-life value of 2-3 minutes (Marx et al., 2000), but not as long as that of human TAFIa of 8 minutes (Hillmayer et al., 2008b). At 25°C, the half-life was estimated to be 12.7 ± 3.5 minutes, which is again shorter than the 45 minutes for human TAFIa (Declerck, 2011). At 0°C, mouse TAFIa was stable, almost indefinitely. Repeated freeze thaw cycles, up to 2 times, did not appear to affect TAFIa function in NMP (Table 2).

3.2 Clot lysis in mouse plasma system

3.2.1 TNK-tPA Optimization

TNK-tPA at varying concentrations was used to identify the concentration that produces a desirable clot lysis time. The clots did not lyse when TNK-tPA levels were below 5 nM, while TNK-tPA levels above 50 nM resulted in premature clot lysis most likely due to excessive Pn generation and fibrin(ogen)olysis. When TNK-tPA levels were varied between 10 and 50 nM, the lysis times (LT) were inversely proportional to the TNK-tPA concentration (Figure 7). Although the overall trend was similar, there was a marked differences in the LT when using fresh NMP compared with previously frozen

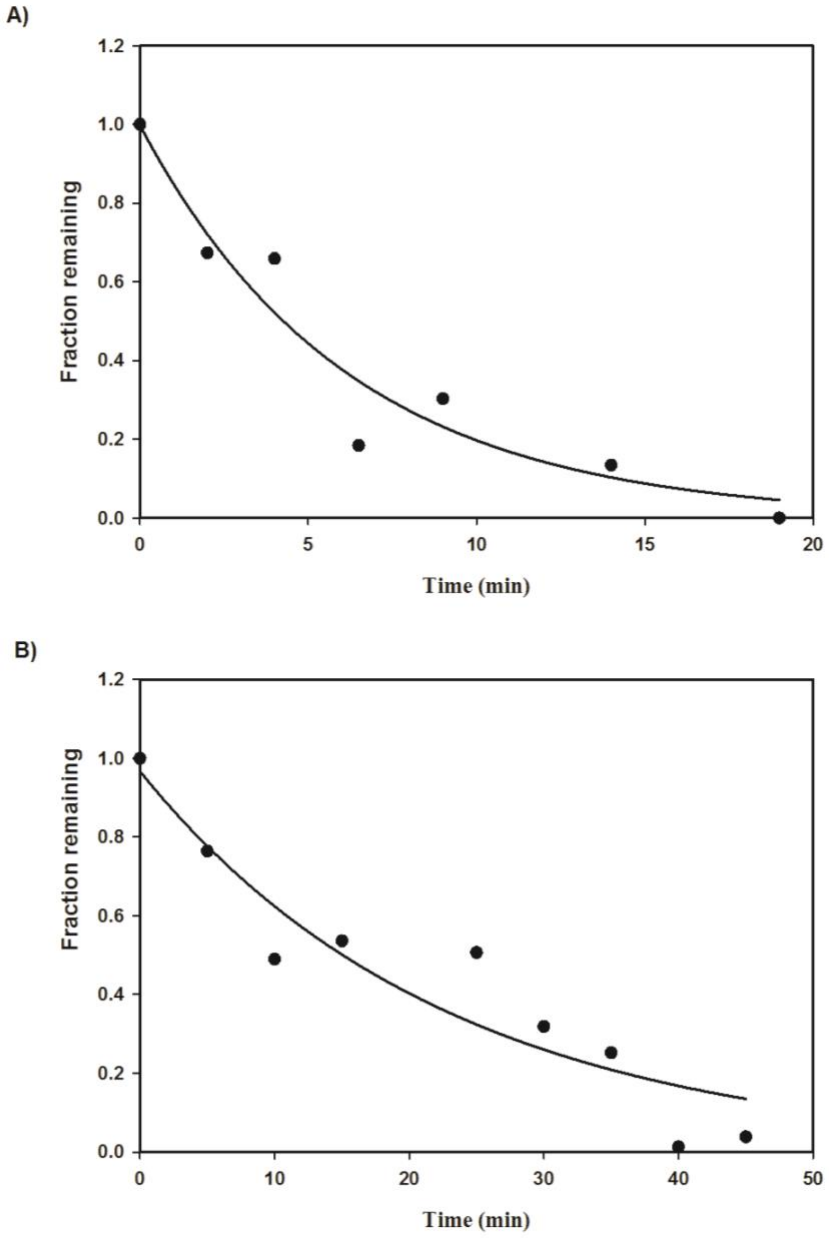

Figure 6. Representative examples of half-life determination at 37 °C (A) and 25 °C (B). TAFI activated mouse serum (using 25 nM thrombin, 100 nM Solulin, 5 mM $CaCl_2$ final) was incubated at 37 °C (A) or 25 °C (B). 50 µL of serum was added to 50 µL of AAFR (280 µM final) at varying times (0 and 20 min). Initial rate at 0 min was considered to be the rate at original amount (V_o) and the initial rates at subsequent time course points (V_t) were expressed as fraction of original amount remaining (V_t/ V_o). Fraction remaining was plotted with respect to time and the data was fitted to first order exponential decay. Time to 0.5 or 50% of original amount remaining was taken as the half-life, 4.5 min (A) or 15.8 min (B).

Table 1. Summary of the determined half-lives of murine TAFIa at 37, 25 and 0 °C (n = 3 each). Mean ± S.D.

Temperature (°C)	Half-life
37	4.0 ± 0.4 min
25	12.7 ± 3.5 min
0	35.0 ± 16.2 h

Table 2. Summary of the activity of mouse TAFIa through freeze-thaw cycles (n = 3 each). Mean ± SD.

Fresh / Freeze-thaw	**Amount remaining (V_{ft}/V_f)**
Fresh	1
Cycle 1	1.07 ± 0.05
Cycle 2	1.05 ± 0.16

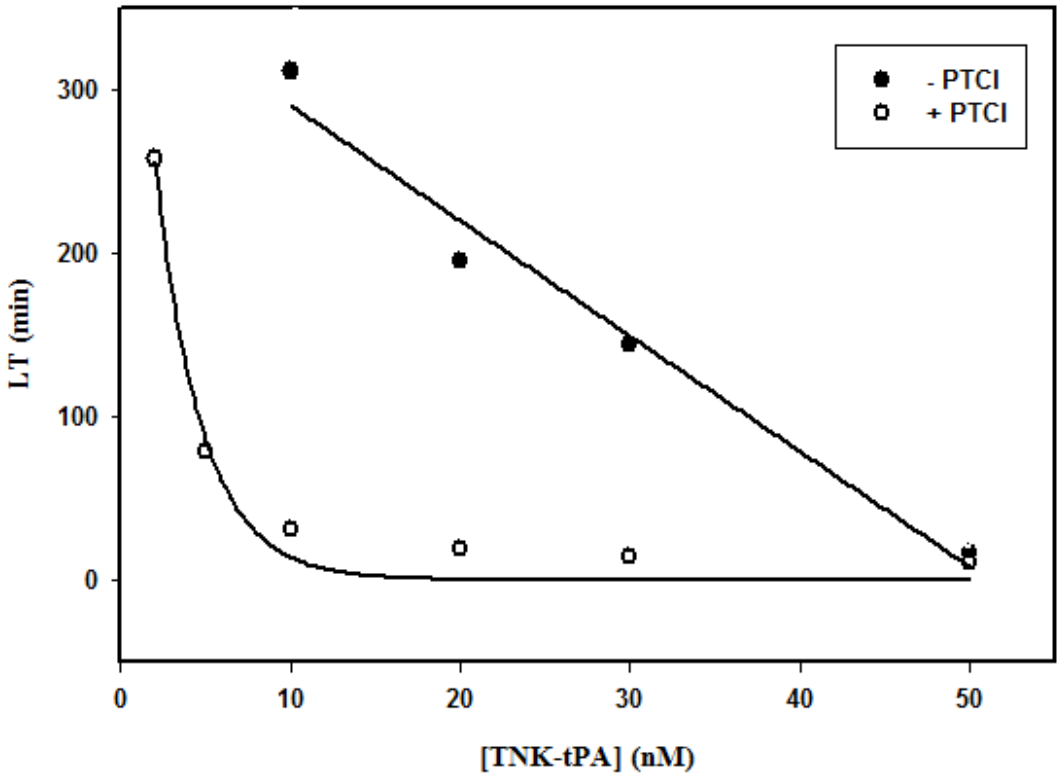

Figure 7. Clot lysis time (LT) of Normal Mouse Plasma (NMP) with varying TNK-tPA concentrations. Plasma was clotted using thrombin and lysis was initiated with TNK-tPA at varying concentrations (0 to 100 nM) at 25°C. The reactions were monitored using turbidity at 400 nm. Time to half-maximal OD change during lysis was taken as the clot lysis time. Lysis times were then plotted with respect to TNK-tPA concentrations used. The regression line represents a line of best fit.

NMP. Clots from previously frozen NMP consistently took longer to lyse compared with fresh NMP at each concentration of TNK-tPA tested. Since the NMP was only frozen for 10 minutes before thawing, the phenomenon is not attributable to reactions or changes that could potentially occur in stored plasma over time.

To avoid the inclusion of more variables and subsequent complications in interpreting the data, only fresh mouse plasma was used in performing the clot lysis assay. Based on the results, 20 nM TNK-tPA was used for subsequent clot lysis assays as this concentration yielded a lysis time of 195.5 minutes. When PTCI was added to the system, LT decreased to 19.1 minutes, suggesting that TAFIa significantly influences the lysis times of mouse plasma clot.

3.2.2 Clot lysis in mouse plasma using optimized TNK-tPA concentration

All mice were catalogued prior to use. WT mice between 5 and 10 weeks of age were significantly heavier compared with both male ApoE$^{-/-}$ and female WT mice of the same age group ($p<0.05$) (Figure 8). Until 15 weeks of age, both male WT and male ApoE$^{-/-}$ mice have increased weight compared to their female counterparts ($p<0.05$). At 30 weeks, the male WT mice remain significantly heavier compared to the male ApoE$^{-/-}$ mice ($p<0.05$). However, all other groups lose any significant differences between them.

LTs of age and sex-matched WT and ApoE$^{-/-}$ mice were compared using the clot lysis assay described using optimized (20 nM) TNK-tPA concentration (Table 3). In the absence of PTCI, no significant differences were observed in the LTs between WT and ApoE$^{-/-}$ (Table 3). Furthermore, LTs of males and females within each age group did not

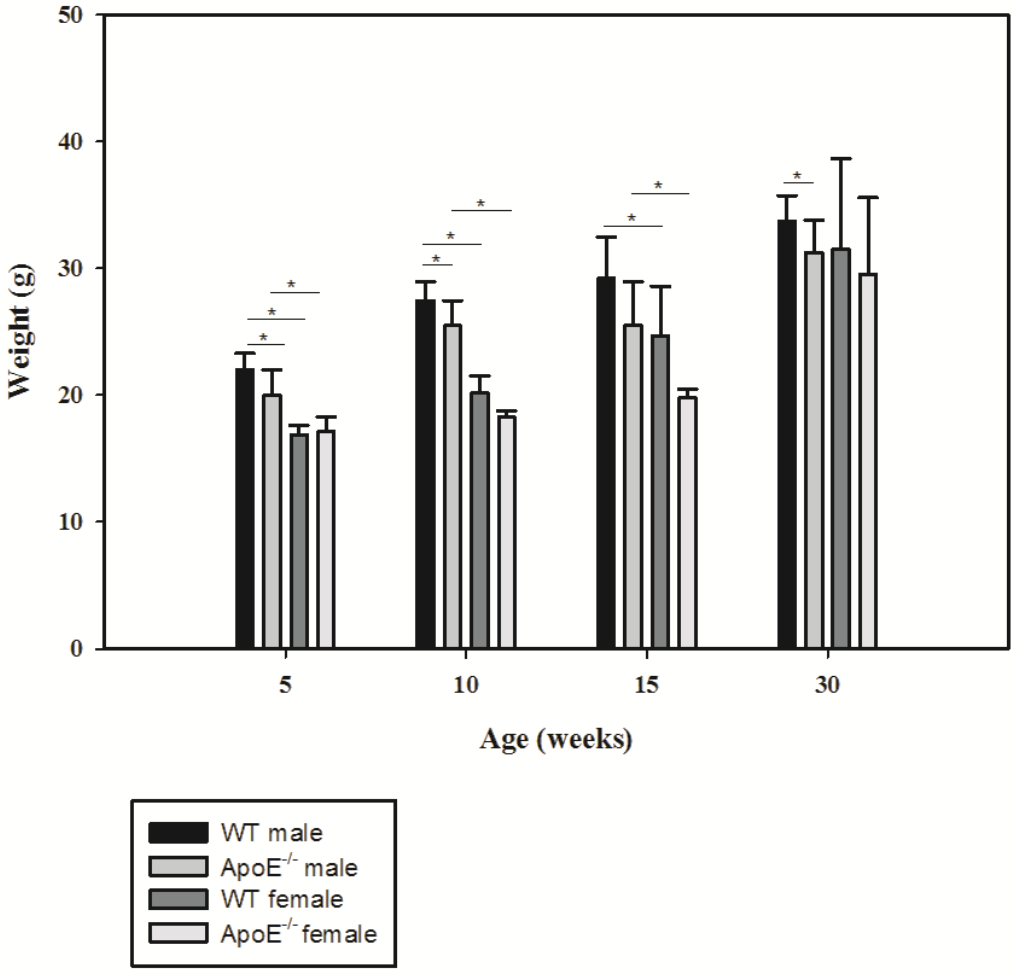

Figure 8. Comparison of the weights of WT and ApoE$^{-/-}$. Overall, WT male mice are heavier than ApoE$^{-/-}$ males and WT females. Males are heavier than the female counterparts in 5, 10, and 15 week categories ($p<0.05$). Data presented as mean ± S.D. Significance ($p<0.05$) indicated with asterisk (*).

differ greatly, demonstrating that sex does not affect LTs in WT or ApoE$^{-/-}$ mice (p=0.532). Even when sex-based stratification was removed, the analysis failed to show any significant differences between WT and ApoE$^{-/-}$ across all age categories (p=0.452).

When PTCI was added to inhibit TAFIa, the LTs decreased prominently across all groups compared with reactions without PTCI (Table 3). Overall, LTs of mice increased significantly across age, without stratifying for genotype or sex ($p<0.002$). ApoE$^{-/-}$ mice, in general, also had increased LTs (20.2 ± 3.4 min), compared with WT (18.28 ± 3.2 min), without accounting for age or sex ($p <0.017$).

Since the LTs appear to be positively correlated with ApoE$^{-/-}$ mice only in the absence of TAFIa (*i.e.* presence of PTCI), it was posited that TAFIa provides a compensatory role in normalizing clot lysis times. To quantify the proportion of compensation that TAFIa provides in each group of mice, ΔLT was calculated and summarized (Table 4). The contribution of TAFIa towards LT, indicated by ΔLT, is reduced in the ApoE$^{-/-}$ mice (8% reduction), especially in the males (12% reduction). Therefore, these data suggest that TAFIa may be compensating for the increased LT in ApoE$^{-/-}$ mice by reducing its influence on LT, thereby achieving normalized lysis times and fibrinolysis in both categories.

As the differences in the baseline (OD_{min}) observed in the plasma samples may be indicative of differences in the composition of plasma while the total turbidity signal change (ΔOD) may be indicative of structural changes in the clots formed, these two parameters were measured from the clot lysis time course profiles. The average OD_{min} of males and females were comparable. The males had a higher average OD_{min} in the 10 and

Table 3. Summary of weights and LTs (with and without PTCI) of WT and ApoE$^{-/-}$ mice. Mean ± S.D.

	Genotype	Age (wks)	Mean LT without PTCI (min)	Mean LT with PTCI (min)	Weight (g)	n
MALES						
	WT	5	211.6 ± 43.9	17.9 ± 0.7	22.0 ± 1.3	4
		10	176.4 ± 21.4	16.5 ± 2.4	27.5 ± 1.5	6
		15	166.5 ± 19.4	14.6 ± 0.11	29.2 ± 3.2	3
		30	207.7 ± 9.4	17.8 ± 1.0	33.7 ± 2.5	4
	ApoE$^{-/-}$	5	164.7 ± 36.9	17.4 ± 0.56	19.9 ± 2.1	6
		10	162.9 ± 30.4	17.6 ± 0.2	25.5 ± 2.0	5
		15	160.6 ± 28.2	17.7 ± 1.5	25.5 ± 3.4	6
		30	196.1 ± 44.7	25.1 ± 1.6	31.3 ± 2.5	3
FEMALE	WT	5	179.1 ± 12.1	15.7 ± 1.5	16.9 ± 0.7	4
		10	205.0 ± 22.1	23.1 ± 3.3	20.2 ± 1.3	4
		15	158.9 ± 28.9	18.9 ± 1.0	24.7 ± 3.9	5
		30	209.1 ± 40.7	21.5 ± 2.9	31.5 ± 7.2	4
	ApoE$^{-/-}$	5	184.7 ± 27.8	19.9 ± 2.8	17.1 ± 1.2	5
		10	186.7 ± 7.7	19.5 ± 2.0	18.3 ± 0.5	4
		15	162.6 ± 26.7	22.1 ± 1.8	19.8 ± 0.7	5
		30	219.6 ± 89.5	24.3 ± 4.1	30.0 ± 6.0	4

Table 4. Summary ΔLTs (with and without PTCI) of WT and ApoE$^{-/-}$ mice. Mean ± S.D.

	Age (wks)	**Mean ΔLT min)**		**ApoE$^{-/-}$/WT**
MALES		WT	ApoE$^{-/-}$	Ratio
	5	188.69	160.04	0.85
	10	163.64	143.45	0.88
	15	152.55	140.03	0.92
	30	189.87	169.90	0.89
	Mean ± SD			**0.88 ± 0.03**
FEMALES				
	5	161.87	164.80	1.02
	10	181.96	147.44	0.81
	15	140.13	140.56	1.00
	30	189.93	195.21	1.03
	Mean ± SD			**0.96 ± 0.1**
ALL MICE				
	Mean ± SD			**0.92 ± 0.08**

30+-week-old ApoE$^{-/-}$ mice compared with WT ($p<0.05$) (Figure 9). The females had significantly higher OD_{min} in the 30+-week-old ApoE$^{-/-}$ group compared with WT ($p<0.05$) (Figure 9). The average ΔOD were greater in the 30+-week age group in ApoE$^{-/-}$ males compared with WT males ($p<0.05$) (Figure 10). The female groups did not statistically differ in average ΔOD (Figure 10).

3.3 Measurement of TAFIa levels in mouse plasma

Mice plasma samples appeared to have an increased apparent background activity in our in-house TAFIa assay compared with human samples. Therefore, the TAFIa assay was performed by using mTDP to make all necessary dilutions for the standards rather than human TDP (Figure 11). Overall, ApoE$^{-/-}$ mice showed decreased apparent TAFIa presence when compared with age/sex-matched WT (Figure 12). The difference was significant only in the 30-week old males ($p<0.05$). The female ApoE$^{-/-}$ mice also exhibited lower levels of TAFIa. The relationship, however, was not significant.

3.3.1 The effect of ApoE$^{-/-}$ plasma in TAFIa assay

Because the plasma samples obtained from the ApoE$^{-/-}$ mice demonstrated abnormally high background signal, the influence of plasma from ApoE$^{-/-}$ mice on the TAFIa activity assay was investigated (Figure 13). When TAFIa standard curves were generated using either mTDP or iAP, the slopes determined were 7.36 RFU/min/pM and 2.83 RFU/min/pM, respectively, suggesting that iAP dampened the apparent TAFIa activity by 2.6-fold. In addition, the y-intercept (*i.e.* apparent base level of TAFIa

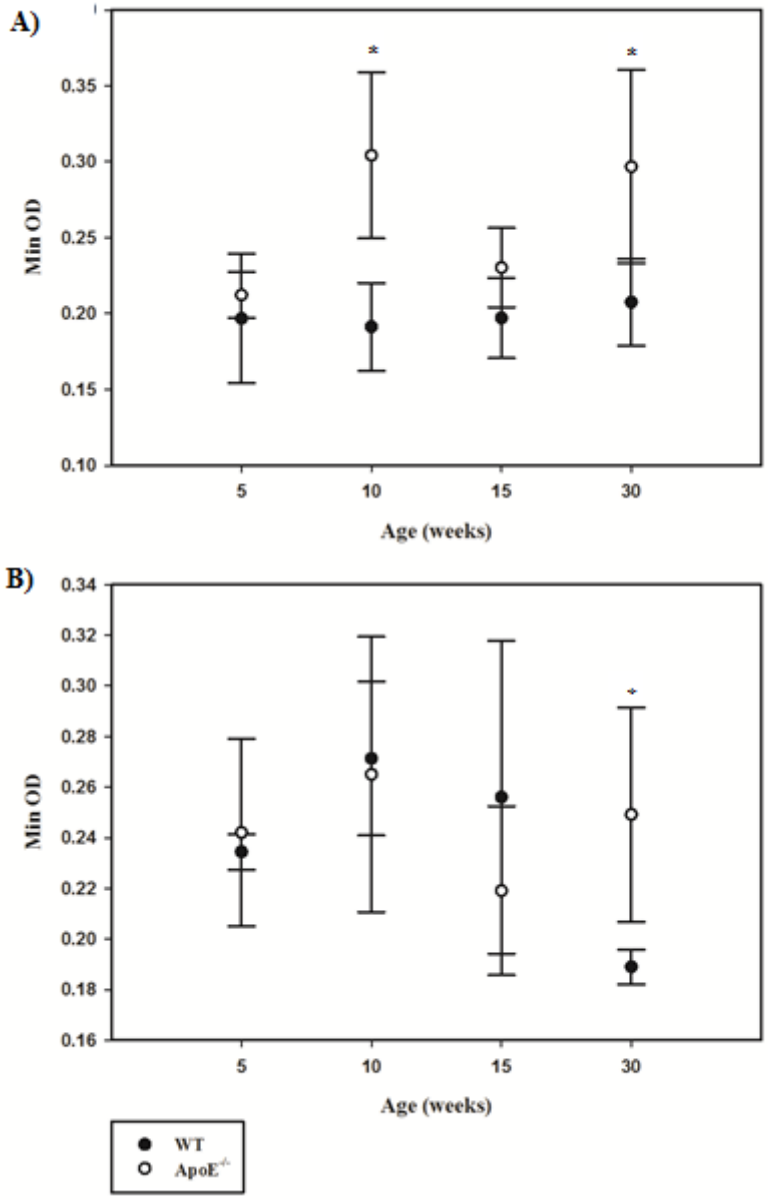

Figure 9. Comparison of the minimum turbidity of samples. The average minimum turbidity or OD_{min} of $ApoE^{-/-}$ mice samples were compared with WT. Minimum OD was plotted against age in the WT and $ApoE^{-/-}$ mice in A) males and B) females. Data presented as mean ± S.D. Significance ($p<0.05$) indicated with asterisk (*).

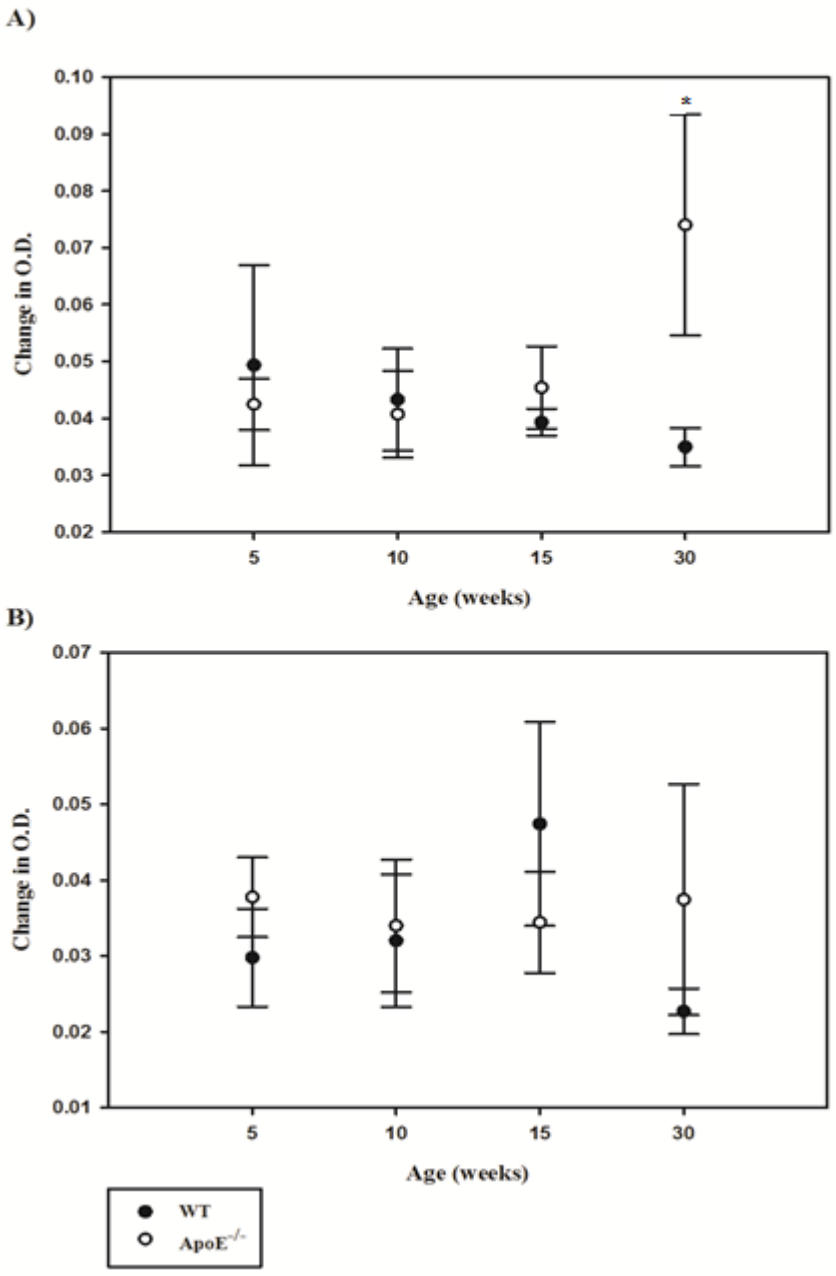

Figure 10. Comparison of total turbidity change of samples. The total turbidity change was determined by subtraction of the minimum O.D. from the maximum O.D.. Change in O.D. was plotted against age in A) males and B) females. Data presented as mean ± S.D. Significance ($p<0.05$) indicated with asterisk (*).

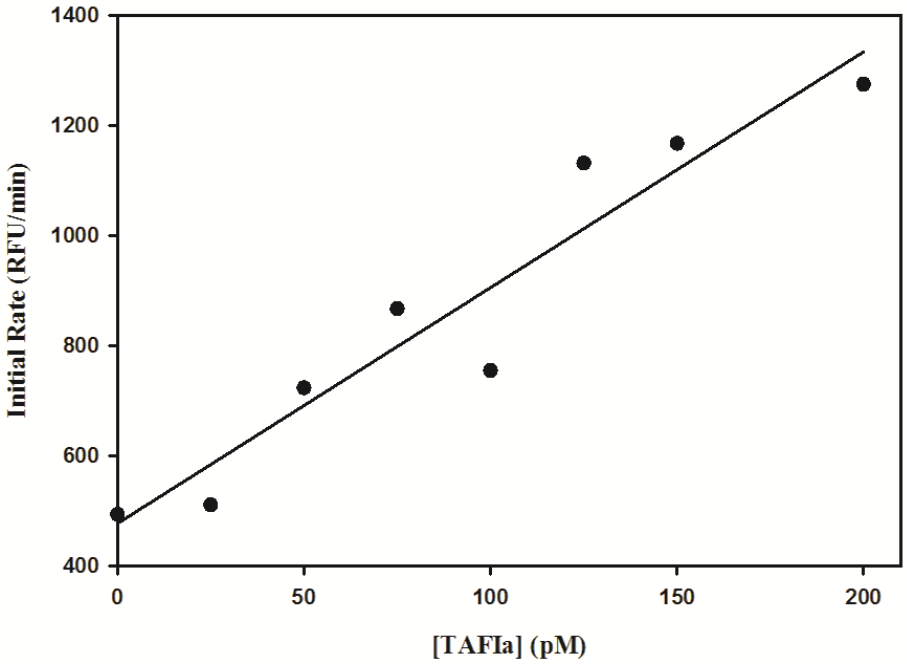

Figure 11. TAFIa standard curve. TAFIa concentrations ranging from 0 to 200 pM final were added to equilibrated QSY-FDPs*●5IAF-Plg mixture (Refer Figure 5). TAFIa cleaves the C-terminal lysine residues (*) thereby dissociating 5IAF-Plg from QSY-FDPs. Dissociation results in fluorescence increase in 5IAF-Plg and the rate of increase is dependent on TAFIa concentration. The initial rates of the known concentration of TAFIa was used to generate a standard curve. Data was fitted to linear regression. The standard curve was then used to quantify unknown concentrations of TAFIa in samples.

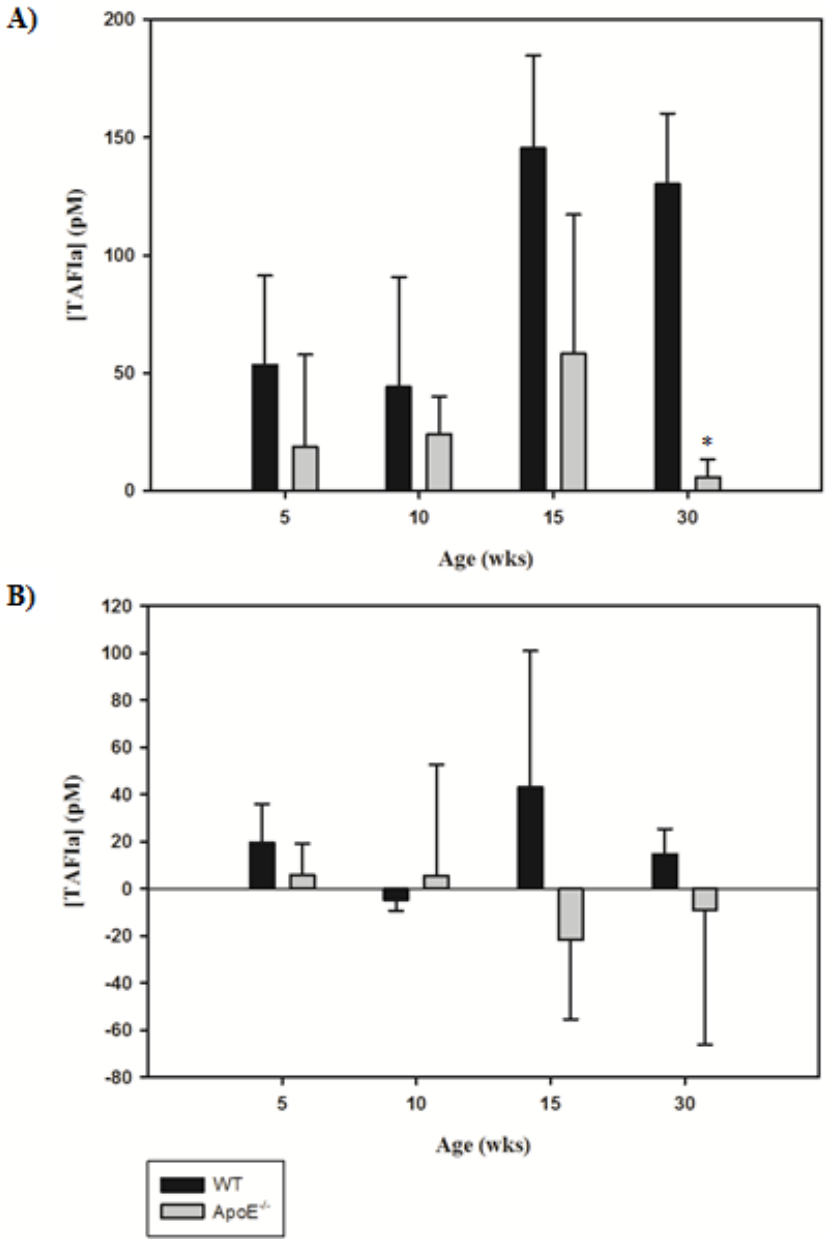

Figure 12. Comparison of TAFIa concentrations between WT and ApoE$^{-/-}$ across age. Plasma samples were added to QSY-FDP*●5IAF-Plg mixture. TAFIa in the samples cleave the C-terminal lysine residues (*) thereby dissociating 5IAF-Plg from QSY-FDPs. Dissociation results in fluorescence increase in 5IAF-Plg and this occurs in a TAFIa-dependent manner. A standard curve with known TAFIa concentrations (0 to 200 pM) generated simultaneously is used to quantify TAFIa in the samples. TAFIa levels in WT mice are compared with age- matched ApoE$^{-/-}$ mice in both A) males and B) females. Data presented as mean ± S.D. Significance ($p<0.05$) indicated with asterisk (*).

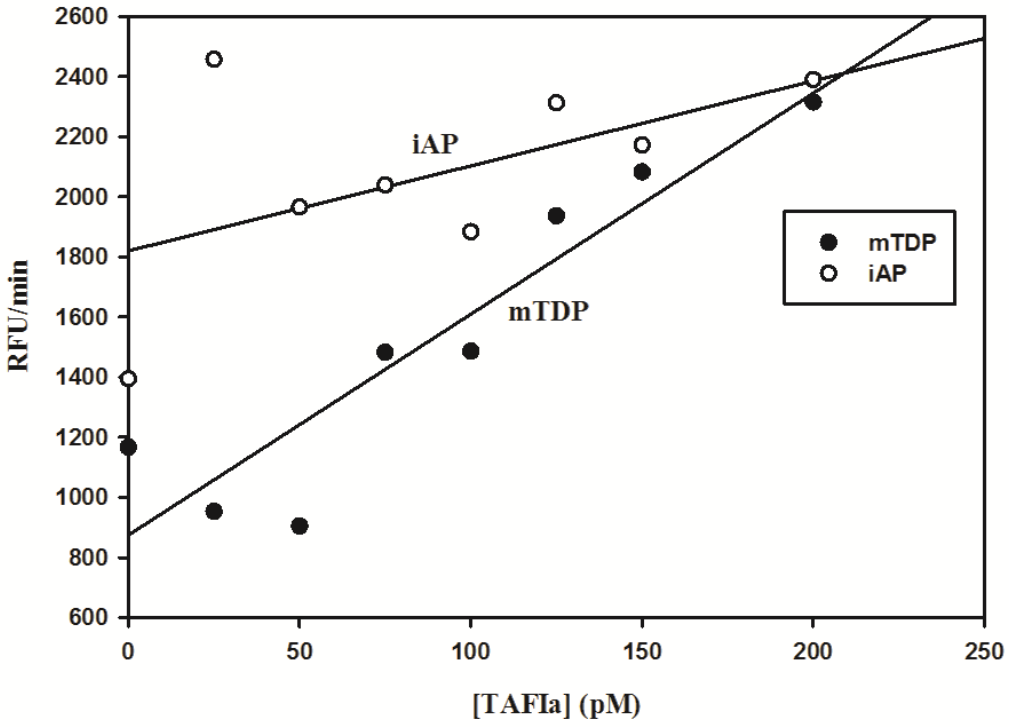

Figure 13. Interference of ApoE$^{-/-}$ plasma in TAFIa assay. TAFIa standard curves (0 to 200 pM) were generated using mTDP (closed circle) and iAP (open circle). The initial rates were plotted against known concentrations of TAFIa. Data was fitted to a linear regression model.

activity) was 2.1-fold higher with iAP (1820.3 RFU/min) than with mTDP (874.2 RFU/min).

3.4 Measurement of TAFI zymogen levels in mouse plasma

Obtained mouse TAFI levels varied between 103 nM to 270 nM. There is a clear overall increase of TAFI zymogen levels with age, within male and female mice of both genotype (Figure 14). The males appear to have higher circulating TAFI levels compared to females. The WT mice also seem to have increased TAFI compared to their $ApoE^{-/-}$ counterpart, especially in males (Figure 14).

3.5 Measurement of inflammatory biomarker levels in mouse plasma

The multiplex assay did not yield any detectable levels of IL-1β, TNF-α, and IL-6. The Quantikine Elisa for measuring mouse IL-10 levels demonstrated very low levels of IL-10 in the plasma samples (Figure 15). IL-10 in $ApoE^{-/-}$ mice was significantly elevated in both males and females of the 15-week age group ($p<0.05$). However, no significant differences were established in the 30-week old mice (Figure 15).

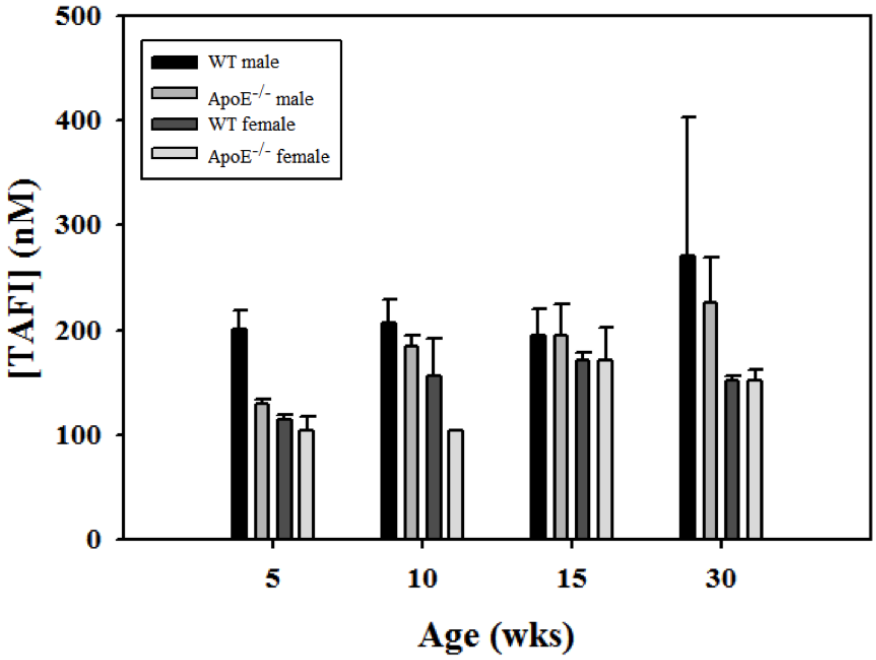

Figure 14. Comparison of TAFI zymogen concentrations between WT and ApoE$^{-/-}$ mice. TAFI concentrations in the mice samples were quantified using mouse TAFI Elisa. TAFI levels in WT mice are compared with age and sex-matched ApoE$^{-/-}$ mice. Data presented as a mean mean ± S.D. (n = 2).

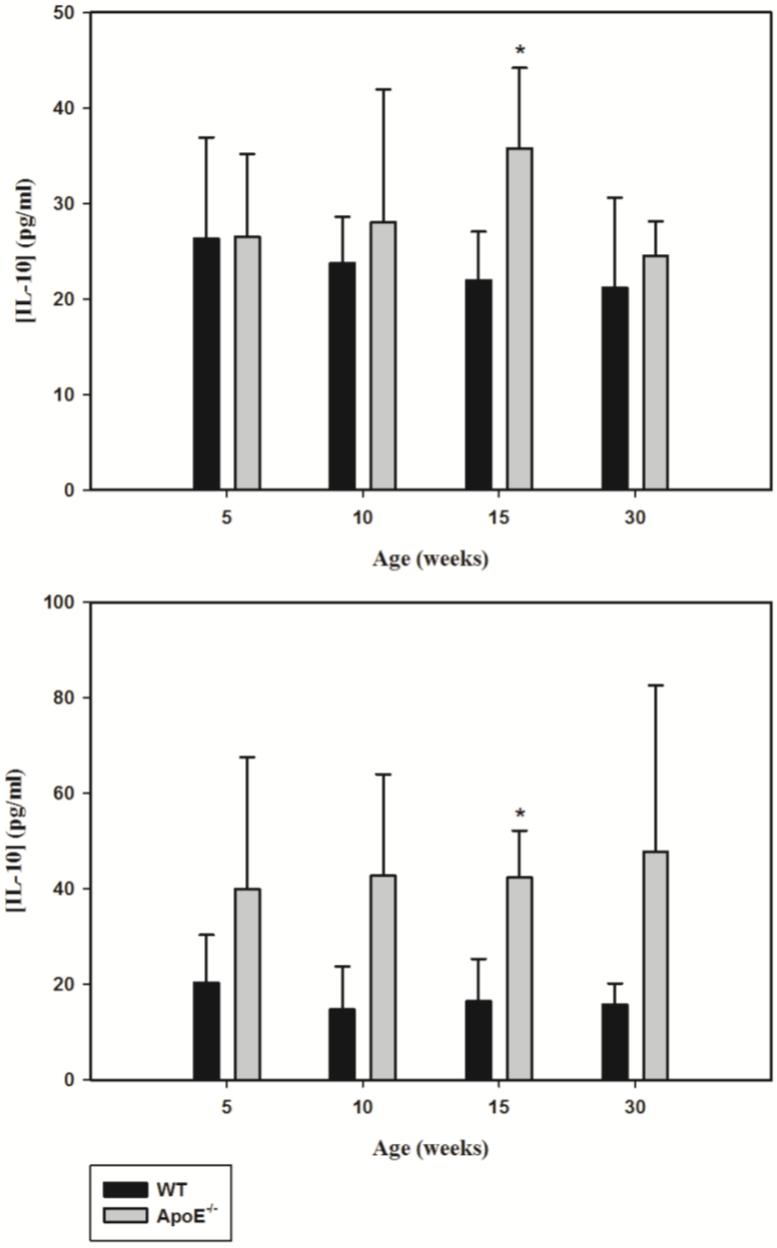

Figure 15. Comparison of IL-10 concentrations between WT and ApoE$^{-/-}$ mice across age. IL-10 concentrations in the mice samples were quantified using mouse IL-10 Elisa. IL-10 levels in WT mice are compared with age- matched ApoE$^{-/-}$ mice in A) males and B) females. Data presented as mean ± S.D. Significance ($p<0.05$) indicated with asterisk (*).

IV. Discussion

The goal of this project was to investigate and identify the potential role of TAFIa in influencing pathogenesis and/or progression of atherosclerosis. Given that both facets of TAFIa activity, anti-inflammatory and antifibrinolytic, are involved in atherosclerosis and atherothrombosis, respectively, it is reasonable to suspect that TAFIa is involved in either or both processes. In the context of influencing fibrinolysis that represents degradation of atherothrombotic clots *in vivo*, our preliminary findings suggested that TAFIa levels are elevated in the ApoE$^{-/-}$ mice compared with the wild-type mice, which results in delayed clot lysis. Our data, however, was unable to show any differences in clot lysis times, demonstrating no attenuation of fibrinolysis in atherosclerotic mice. The delayed LTs in ApoE$^{-/-}$ mice compared to WT, with the inclusion of PTCI, may be due to factors other than TAFIa that could affect fibrinolysis. For instance, ApoE$^{-/-}$ mice have increased plasma lipid levels that could play a role in fibrinolysis attenuation. It has previously been shown that fibrinolysis is attenuated with increased lipid levels (Holvoet & Collen, 1995). Despite the greater delay in the LTs in ApoE$^{-/-}$ mice, the differences were minimal in the absence of PTCI, suggesting that TAFIa is able to compensate to normalize these minimal differences so that fibrinolysis, or LTs, is comparable across the ages.

When the mice plasma samples were measured spectrometrically, although not statistically significant, there was a trend of increasing OD_{min} in ApoE$^{-/-}$ mice samples with increasing age, with greatest separation from the WT in the 30+ week old male mice. This could indicate increasing lipid concentrations with age in ApoE$^{-/-}$ mice, an observation consistent with a clinical study that showed a positive correlation between serum turbidity

and increased triglyceride levels, albeit the findings being based on visual inspection and not spectrophotometric analyses (Lim, Lian, & Yeo, 2006). While the female 30+ week old ApoE$^{-/-}$ mice may have higher OD_{min} compared with the WT, the significance is uncertain as the mean OD_{min} values of other age groups for both the WT and ApoE$^{-/-}$ mice are similar.

Furthermore, increased ΔOD values were observed in the 30+ week old ApoE$^{-/-}$ male mice, suggesting that there could be structural differences in these clots compared with other age groups and/or sex. While the turbidity change is not specific enough to identify the cause of structural change in the clot, previous studies have shown that the presence of cell-free DNA, fibrinogen levels, and thrombin levels all may influence the polymerization process (Gould et al., 2015).

Direct measurement of TAFIa in our samples showed that the apparent TAFIa levels were decreased in the atherosclerotic mice. Moreover, female ApoE$^{-/-}$ mice exhibited negative mean TAFIa values, suggesting that the functionality of the TAFIa assay may be compromised with these samples. The phenomenon could be due to a possible interference in the binding of 5IAF-Plg to QSY-FDPs. Cholesterol is a potential molecule that could be causing this effect, especially in the ApoE$^{-/-}$ plasmas. ApoE$^{-/-}$ mice have high plasma cholesterol levels ranging between 400 to 600 mg/dl compared with 75 to 110 mg/dl in the WT mice (Nakashima et al., 1994; Plump & Breslow, 1995). The females may have increased cholesterol/lipid levels, particularly in the 15 and 30-week age groups resulting in increased interference in this assay. The lipid levels at these age categories have not been established or stratified based on sex. A possible mechanism of cholesterol interference

involves apolipoprotein A (ApoA) which shares structural similarities to plasminogen (Hancock, Boffa, Marcovina, Nesheim, & Koschinsky, 2003). Similar to Plg, ApoA has lysine-binding sites on its kringle domains that are capable of binding to lysine residues on Fgn and/or FDPs. Therefore, apoA could compete with Plg for the lysine residues on the QSY-FDPs. However, ApoA is mostly carried on high density lipoproteins, which is greatly decreased in $ApoE^{-/-}$ mice (Moghadasian et al., 2001). The role of other apolipoproteins in this interference remains to be investigated.

The apparent levels of TAFIa activity when the standard curve was generated using mTDP was consistently higher than when normal human TDP was used. It is unclear if mice carboxypeptidase N has the ability to cleave lysine residues on plasmin-modified fibrin and this in turn contributes to the increased baseline readings. It is also possible that mouse Plg binds QSY-FDPs with a higher affinity and compete for the same binding sites against 5IAF-Plg, which would displace 5IAF-Plg and result in higher apparent TAFIa activity. It is also not known if there may be another carboxypeptidase in mice plasma that can remove lysine residues similar to that of TAFIa. Further investigation needs to be conducted to elucidate the source of the interference in this assay when measuring mouse plasma samples.

In addition to the high background activity in mice plasma, $ApoE^{-/-}$ mice plasma further affects the TAFIa assay. The decreasing sensitivity of the assay (Figure 14) to increasing TAFIa concentrations (in iAP standard curve), demonstrates a clear inference in the assay. It is important to note that iAP has an increased baseline initial rate, compared to mTDP, when there is no TAFIa present in the system (Figure 14). It is important to note

that even with this increased baseline, the TAFIa concentrations are decreased in ApoE$^{-/-}$ mice samples compared with WT (Figure 13). This could suggest that TAFIa may in fact be decreased in ApoE$^{-/-}$ mice. This, however, cannot be concluded due to the interference of ApoE$^{-/-}$ samples with this assay.

The TAFI zymogen levels quantified from the assay were higher compared to that reported by Hillmayer *et al* (Hillmayer et al., 2008a). The C57BL/6J mice in the study are shown to have an average of 68 nM plasma concentration of TAFI. The ages and sex of the mice have not been reported. Our study shows a higher concentration of TAFI, about 158 nM, in 5 week old WT mice. Though higher, the values are comparable to the human concentration of TAFI, varying between 73 to 250 nM in circulation (Bajzar et al., 1995). The increasing TAFI concentration with age is an important trend to look at, especially among male WT mice. The increasing TAFI with age is paralleled with increasing TAFIa concentrations, suggesting that increased baseline TAFI levels can contribute to increased TAFI activation.

Measurement of cytokine levels such as IL-6 and IL-10 are often used as an indicator of inflammatory state in cells and animals. It is reasonable to expect IL-10 levels to increase during inflammatory stages, at least in the ApoE$^{-/-}$ mice, in order to combat the increasing proinflammatory cytokines (Han & Boisvert, 2015; Schneider, Schwacha, & Chaudry, 2004). This is supported by a study that found elevated levels of IL-10 in osteoarthritis of the knee and fibromyalgia (Imamura et al., 2014). IL-10 levels in our study also appear to be increased in atherosclerotic mice. One plausible mechanism for this increase involves the interaction between IL-1 and IL-10 (Manzanillo, Eidenschenk, &

Ouyang, 2015). IL-1 and IL-10 families have shown to impact each other's production pleiotropically within the gut (Manzanillo et al., 2015). This interaction may also be happening in $ApoE^{-/-}$ mice where macrophages secrete cytokines including IL-1 to amplify the immune response within a plaque, ultimately resulting in increased IL-10 production to counteract and inhibit IL-1. Nevertheless, further investigation is required to decipher the cytokine networking in inflammatory conditions.

Our model of $ApoE^{-/-}$ mice could have been unsuitable to study TAFIa elevation in atherosclerosis. As the major function of TAFIa is thought to be attenuating fibrinolysis, it is reasonable that the major role of TAFIa is involved in influencing degradation of microthrombi/thrombi that form within atherosclerotic lesions or ruptured plaques. The difficulty in investigating the role of TAFIa in influencing atherothrombosis in mice is that there are no reliable models available for this purpose. Although Welch *et al.* (Welch et al., 2007) have reported that a double knockout variant ($ApoE^{-/-}$ and $Npc1^{-/-}$) with a defect in cholesterol transport allowed for plaque complication leading to spontaneous thrombi formation, these mice are not readily available. Alternatively, a novel model was described at a Gordon Hemostasis Conference (2016) by Heestermans *et al.* (Leiden University Medical Center, the Netherlands) whereby a small interfering RNA targeting protein C expression is able to trigger the formation of spontaneous atherosclerotic lesions with superimposing thrombi in $ApoE^{-/-}$ mice, at a low incidence rate of about 25% (Ouweneel et al., 2017). We could utilize this model for our purposes in investigating the role of TAFI(a) in influencing atherothrombosis in these mice. $ApoE^{-/-}C1039G^{+/-}$ mice are another potential model that could be used for our purposes. These $ApoE^{-/-}$ mice have reduced

fibrinilin-1, which is a glycoprotein that provides a scaffold for the deposition and the cross-linking of elastin. Impaired elastin structure on the artery wall could lead to unstable plaques, resulting in endpoints such as myocardial infarction and sudden death. The advantage of this model is that these end points could only occur when the mice are fed western-type diet, which is analogous to high-fat diet exacerbated atherosclerosis and related end points in humans (Van Herck et al., 2009).

What is uncertain, however, is the mechanism by which TAFI activation could be enhanced. While it is possible that the development of atherosclerotic lesions generates a procoagulant environment that leads to thrombin accumulation and consequently TAFI activation, this has not been demonstrated to date. Furthermore, a key hallmark characteristic of the $ApoE^{-/-}$ mice is that their plasma lipid levels are greatly increased. Since increased lipids in circulation have been linked to reduced fibrinolysis (Holvoet et al., 1995), lipid modulation could be one mechanism by which TAFI activation is enhanced.

Currently there are no biomarkers that can be used clinically to detect early onset of atherosclerosis. The activation of TAFI and the consequent, detection of elevated TAFIa in plasma could be indicative of an on-going process as the presence of elevated levels of TAFIa are transient. In addition, there are no known inhibitors of TAFIa in circulation while its intrinsic half-life at 37°C is under 8 minutes (Schneider et al., 2002). This short half-life of TAFIa provides a distinct advantage as this could not be used to identify ongoing acute inflammatory response, which affects inflammatory biomarkers. A chronic inflammatory disease like atherosclerosis could provide the conditions for sustained

elevated TAFIa levels, even with its limited half-life. Investigation into the potential predictive relationship between TAFIa and atherosclerosis progression can lead to TAFIa becoming a potential biomarker for atherosclerosis. If confirmed, we will be able to invest more in early detection and treatment of atherosclerosis.

V. Future directions

To investigate if reduced fibrinolysis upon elevated lipids in circulation is TAFI(a)-dependent, we will characterize TAFI activation time-course in the plasma of $ApoE^{-/-}$ and WT mice during clot formation and lysis using our in-house TAFIa assay.

To elucidate the role of TAFI(a) in atherosclerosis, we will generate and characterize ApoE/TAFI double knock-out mice. The atherosclerotic lesions in these mice will be then compared to that of $ApoE^{-/-}$ mice.

While TAFIa may not be involved in general atherosclerosis, it could be elevated in diabetes accelerated atherosclerosis where fibrinolysis is greatly attenuated. We will utilize $ApoE^{-/-}$:$Ins2^{+/Akita}$, which are mice associated with type-1 diabetes phenotype, and compare their clot lysis times and TAFIa levels to age and sex-matched wild-type mice. We will also be using alternative models to study the role of TAFIa in atherothrombosis, as discussed previously.

VI. Reference List

Acharji, S., Lakshmanadoss, U., Rudzinski, W., Stapleton, D. D., & Kaluski, E. (2013). Use of antiplatelet agents in patients with atherosclerotic disease. *Postgrad.Med., 125,* 19-30.

Ammirati, E., Moroni, F., Norata, G. D., Magnoni, M., & Camici, P. G. (2015). Markers of inflammation associated with plaque progression and instability in patients with carotid atherosclerosis. *Mediators.Inflamm., 2015,* 718329.

Bajzar, L., Manuel, R., & Nesheim, M. E. (1995). Purification and characterization of TAFI, a thrombin-activable fibrinolysis inhibitor. *Journal of Biological Chemistry, 270,* 14477-14484.

Bicakcigil, M., Tasan, D., Tasdelen, N., Mutlu, N., & Yavuz, S. (2011). Role of fibrinolytic parameters and plasminogen activator inhibitor 1 (PAI-1) promoter polymorphism on premature atherosclerosis in SLE patients. *Lupus, 20,* 1063-1071.

Bruunsgaard, H., Skinhoj, P., Pedersen, A. N., Schroll, M., & Pedersen, B. K. (2000). Ageing, tumour necrosis factor-alpha (TNF-alpha) and atherosclerosis. *Clinical and Experimental Immunology, 121,* 255-260.

Campbell, W. D., Lazoura, E., Okada, N., & Okada, H. (2002). Inactivation of C3a and C5a octapeptides by carboxypeptidase R and carboxypeptidase N. *Microbiol.Immunol., 46,* 131-134.

Castellino, F. J. & Powell, J. R. (1981). Human plasminogen. *Methods in Enzymology, 80 Pt C,* 365-378.

Castillo, L., Rohatgi, A., Ayers, C. R., Owens, A. W., Das, S. R., Khera, A. et al. (2010). Associations of four circulating chemokines with multiple atherosclerosis phenotypes in a large population-based sample: results from the dallas heart study. *J.Interferon Cytokine Res., 30,* 339-347.

Cesari, M., Penninx, B. W., Newman, A. B., Kritchevsky, S. B., Nicklas, B. J., Sutton-Tyrrell, K. et al. (2003). Inflammatory markers and onset of cardiovascular events: results from the Health ABC study. *Circulation, 108,* 2317-2322.

Chapin, J. C. & Hajjar, K. A. (2015). Fibrinolysis and the control of blood coagulation. *Blood Reviews, 29,* 17-24.

Corrado, E., Rizzo, M., Coppola, G., Fattouch, K., Novo, G., Marturana, I. et al. (2010). An update on the role of markers of inflammation in atherosclerosis. *J.Atheroscler.Thromb., 17,* 1-11.

Couper, K. N., Blount, D. G., & Riley, E. M. (2008). IL-10: the master regulator of immunity to infection. *J.Immunol., 180,* 5771-5777.

Cybulsky, M. I., Iiyama, K., Li, H., Zhu, S., Chen, M., Iiyama, M. et al. (2001). A major role for VCAM-1, but not ICAM-1, in early atherosclerosis. *J.Clin.Invest, 107,* 1255-1262.

Declerck, P. J. (2011). Thrombin activatable fibrinolysis inhibitor. *Hamostaseologie., 31,* 165-173.

Dhurat, R. & Sukesh, M. (2014). Principles and Methods of Preparation of Platelet-Rich Plasma: A Review and Author's Perspective. *J.Cutan.Aesthet.Surg., 7,* 189-197.

Duguid, J. B. (1946). Thrombosis as a factor in the pathogenesis of coronary atherosclerosis. *J.Pathol.Bacteriol., 58,* 207-212.

Eaton, D. L., Malloy, B. E., Tsai, S. P., Henzel, W., & Drayna, D. (1991). Isolation, Molecular Cloning, and Partial Characterization of a Novel Carboxypeptidase B from Human Plasma. Journal of Biological Chemistry 266, 21833-21838.

Eitzman, D. T., Westrick, R. J., Xu, Z., Tyson, J., & Ginsburg, D. (2000). Plasminogen activator inhibitor-1 deficiency protects against atherosclerosis progression in the mouse carotid artery. *Blood, 96,* 4212-4215.

Elkind, M. S., Cheng, J., Boden-Albala, B., Rundek, T., Thomas, J., Chen, H. et al. (2002). Tumor necrosis factor receptor levels are associated with carotid atherosclerosis. *Stroke, 33,* 31-37.

Fernandes, A. B., Lima, L. M., Sousa, M. O., Toledo, V. P., Kazmi, R. S., Lwaleed, B. A. et al. (2015). Impaired fibrinolysis in angiographically documented coronary artery disease. *Adv.Hematol., 2015,* 214680.

Flacke, S., Fischer, S., Scott, M. J., Fuhrhop, R. J., Allen, J. S., McLean, M. et al. (2001). Novel MRI contrast agent for molecular imaging of fibrin: implications for detecting vulnerable plaques. *Circulation, 104,* 1280-1285.

Foley, J. H., Kim, P. Y., Mutch, N. J., & Gils, A. (2013). Insights into thrombin activatable fibrinolysis inhibitor function and regulation. *Journal of Thrombosis & Haemostasis, 11 Suppl 1,* 306-315.

Fricker, L. D., Plummer, T. H., Jr., & Snyder, S. H. (1983). Enkephalin convertase: potent, selective, and irreversible inhibitors. *Biochem.Biophys.Res.Commun., 111,* 994-1000.

Furie, M. B. & Mitchell, R. N. (2012). Plaque attack: one hundred years of atherosclerosis in The American Journal of Pathology. *American Journal of Pathology, 180,* 2184-2187.

Germolec, D. R., Shipkowski, K. A., Frawley, R. P., & Evans, E. (2018). Markers of Inflammation. *Methods Mol.Biol., 1803,* 57-79.

Getz, G. S. & Reardon, C. A. (2012). Animal models of atherosclerosis. *Arterioscler.Thromb.Vasc.Biol., 32,* 1104-1115.

Getz, G. S. & Reardon, C. A. (2016). Do the Apoe-/- and Ldlr-/- Mice Yield the Same Insight on Atherogenesis? *Arterioscler.Thromb.Vasc.Biol., 36,* 1734-1741.

Gopal, D. M., Larson, M. G., Januzzi, J. L., Cheng, S., Ghorbani, A., Wollert, K. C. et al. (2014). Biomarkers of cardiovascular stress and subclinical atherosclerosis in the community. *Clinical Chemistry, 60,* 1402-1408.

Gould, T. J., Vu, T. T., Stafford, A. R., Dwivedi, D. J., Kim, P. Y., Fox-Robichaud, A. E. et al. (2015). Cell-Free DNA Modulates Clot Structure and Impairs Fibrinolysis in Sepsis. *Arterioscler.Thromb.Vasc.Biol., 35,* 2544-2553.

Han, X. & Boisvert, W. A. (2015). Interleukin-10 protects against atherosclerosis by modulating multiple atherogenic macrophage function. *Thrombosis & Haemostasis, 113,* 505-512.

Hancock, M. A., Boffa, M. B., Marcovina, S. M., Nesheim, M. E., & Koschinsky, M. L. (2003). Inhibition of plasminogen activation by lipoprotein(a): critical domains in apolipoprotein(a) and mechanism of inhibition on fibrin and degraded fibrin surfaces. *Journal of Biological Chemistry, 278,* 23260-23269.

Henderson, S. J., Weitz, J. I., & Kim, P. Y. (2018). Fibrinolysis: strategies to enhance the treatment of acute ischemic stroke. *Journal of Thrombosis & Haemostasis*.

Hillmayer, K., Brouwers, E., Leon-Tamariz, F., Meijers, J. C., Marx, P. F., Declerck, P. J. et al. (2008a). Development of sandwich-type ELISAs for the quantification of rat and murine thrombin activatable fibrinolysis inhibitor in plasma. *Journal of Thrombosis & Haemostasis, 6,* 132-138.

Hillmayer, K., Ceresa, E., Vancraenenbroeck, R., Declerck, P. J., & Gils, A. (2008b). Conformational (in)stability of rat vs. human activated thrombin activatable fibrinolysis inhibitor. *Journal of Thrombosis & Haemostasis, 6,* 1426-1428.

Hirano, K., Young, S. G., Farese, R. V., Jr., Ng, J., Sande, E., Warburton, C. et al. (1996). Targeted disruption of the mouse apobec-1 gene abolishes apolipoprotein B mRNA editing and eliminates apolipoprotein B48. *Journal of Biological Chemistry, 271,* 9887-9890.

Holvoet, P. & Collen, D. (1995). Lipid lowering and enhancement of fibrinolysis with niacin. *Circulation, 92,* 698-699.

Hong, S. N., Gona, P., Fontes, J. D., Oyama, N., Chan, R. H., Kenchaiah, S. et al. (2013). Atherosclerotic biomarkers and aortic atherosclerosis by cardiovascular magnetic resonance imaging in the Framingham Heart Study. *J.Am.Heart Assoc., 2,* e000307.

Horrevoets, A. J., Pannekoek, H., & Nesheim, M. E. (1997). A steady-state template model that describes the kinetics of fibrin-stimulated [Glu1]- and [Lys78]plasminogen activation by native tissue-type plasminogen activator and variants that lack either the finger or kringle-2 domain. *Journal of Biological Chemistry, 272,* 2183-2191.

Hoyer-Hansen, G., Ronne, E., Solberg, H., Behrendt, N., Ploug, M., Lund, L. R. et al. (1992). Urokinase Plasminogen Activator Cleaves Its Cell Surface Receptor Releasing the Ligand-binding Domain. *Journal of Biological Chemistry, 267,* 18224-18229.

Hoylaerts, M., Rijken, D. C., Lijnen, H. R., & Collen, D. (1982). Kinetics of the activation of plasminogen by human tissue plasminogen activator. Role of fibrin. *Journal of Biological Chemistry, 257,* 2912-2919.

Idriss, H. T. & Naismith, J. H. (2000). TNF alpha and the TNF receptor superfamily: structure-function relationship(s). *Microsc.Res.Tech., 50,* 184-195.

Imamura, M., Targino, R. A., Hsing, W. T., Imamura, S., Azevedo, R. S., Boas, L. S. et al. (2014). Concentration of cytokines in patients with osteoarthritis of the knee and fibromyalgia. *Clin.Interv.Aging, 9,* 939-944.

Iwaki, T., Sandoval-Cooper, M. J., Brechmann, M., Ploplis, V. A., & Castellino, F. J. (2006). A fibrinogen deficiency accelerates the initiation of LDL cholesterol-driven atherosclerosis via thrombin generation and platelet activation in genetically predisposed mice. *Blood, 107,* 3883-3891.

Jenny, N. S., Brown, E. R., Detrano, R., Folsom, A. R., Saad, M. F., Shea, S. et al. (2010). Associations of inflammatory markers with coronary artery calcification: results from the Multi-Ethnic Study of Atherosclerosis. *Atherosclerosis, 209,* 226-229.

Kaczmarek, E., Lee, M. H., & McDonagh, J. (1993). Initial interaction between fibrin and tissue plasminogen activator (t-PA). The Gly-Pro-Arg-Pro binding site on fibrin(ogen) is important for t-PA activity. *Journal of Biological Chemistry, 268,* 2474-2479.

Kalafatis, M., Egan, J. O., van, '., V, Cawthern, K. M., & Mann, K. G. (1997). The regulation of clotting factors. *Crit Rev.Eukaryot.Gene Expr., 7,* 241-280.

Kim, P. Y., Foley, J., Hsu, G., Kim, P. Y., & Nesheim, M. E. (2008). An assay for measuring functional activated thrombin-activatable fibrinolysis inhibitor in plasma. *Analytical Biochemistry, 372,* 32-40.

Klement, P., Liao, P., & Bajzar, L. (1999). A novel approach to arterial thrombolysis. *Blood, 94,* 2735-2743.

Kremen, M., Krishnan, R., Emery, I., Hu, J. H., Slezicki, K. I., Wu, A. et al. (2008). Plasminogen mediates the atherogenic effects of macrophage-expressed urokinase and accelerates atherosclerosis in apoE-knockout mice. *Proc.Natl.Acad.Sci.U.S.A, 105,* 17109-17114.

Lammeren, W. v., Moll, L., Borst, G. J., de Kleijn, D. P., Vries JP, P. M., & Pasterkamp, G. (2011). Atherosclerotic plaque biomarkers: beyond the horizon of the vulnerable plaque. *Curr.Cardiol.Rev., 7,* 22-27.

Lee, S. G., Kalyan, N., Wilhelm, J., Hum, W. T., Rappaport, R., Cheng, S. M. et al. (1988). Construction and Expression of Hybrid Plasminogen Activators Prepared from Tissue-type Plasminogen Activator and Urokinase-type Plasminogen Activator Genes. *Journal of Biological Chemistry, 263,* 2917-2924.

Leebeek, F. W., Goor, M. P., Guimaraes, A. H., Brouwers, G. J., Maat, M. P., Dippel, D. W. et al. (2005). High functional levels of thrombin-activatable fibrinolysis inhibitor are associated with an increased risk of first ischemic stroke. *Journal of Thrombosis & Haemostasis, 3,* 2211-2218.

Leung, L. L., Nishimura, T., & Myles, T. (2008). Regulation of tissue inflammation by thrombin-activatable carboxypeptidase B (or TAFI). *Advances in Experimental Medicine & Biology, 632,* 61-69.

Ley, K., Miller, Y. I., & Hedrick, C. C. (2011). Monocyte and macrophage dynamics during atherogenesis. *Arterioscler.Thromb.Vasc.Biol., 31,* 1506-1516.

Li, Y., Zeng, Z., Zhao, J., Ma, G., Cui, L., Tao, H. et al. (2014). Association between polymorphisms in the flanking region of the TAFI gene and atherosclerotic cerebral infarction in a Chinese population. *Lipids Health Dis., 13,* 80.

Libby, P. (2017). Interleukin-1 Beta as a Target for Atherosclerosis Therapy: Biological Basis of CANTOS and Beyond. *Journal of the American College of Cardiology, 70,* 2278-2289.

Lim, K. H., Lian, W. B., & Yeo, C. L. (2006). Does visual turbidity correlate with serum triglyceride levels in babies on total parenteral nutrition? *Ann.Acad.Med.Singapore, 35,* 790-793.

Lin, J. H., Garand, M., Zagorac, B., Schadinger, S. L., Scipione, C., Koschinsky et al. (2011). Identification of human thrombin-activatable fibrinolysis inhibitor in vascular and inflammatory cells. *Thrombosis & Haemostasis, 105,* 999-1009.

Lo, S. G., Schlage, W. K., Boue, S., Veljkovic, E., Peitsch, M. C., & Hoeng, J. (2016). The Apoe(-/-) mouse model: a suitable model to study cardiovascular and respiratory diseases in the context of cigarette smoke exposure and harm reduction. *J.Transl.Med., 14,* 146.

Lusis, A. J. (2000). Atherosclerosis. *Nature, 407,* 233-241.

Mallat, Z., Besnard, S., Duriez, M., Deleuze, V., Emmanuel, F., Bureau, M. F. et al. (1999). Protective role of interleukin-10 in atherosclerosis. *Circulation Research, 85,* e17-e24.

Manzanillo, P., Eidenschenk, C., & Ouyang, W. (2015). Deciphering the crosstalk among IL-1 and IL-10 family cytokines in intestinal immunity. *Trends Immunol., 36,* 471-478.

Mao, S. S., Cooper, C. M., Wood, T., Shafer, J. A., & Gardell, S. J. (1999). Characterization of plasmin-mediated activation of plasma procarboxypeptidase B. Modulation by glycosaminoglycans. *Journal of Biological Chemistry, 274,* 35046-35052.

Marx, P. F., Wagenaar, G. T., Reijerkerk, A., Tiekstra, M. J., van Rossum, A. G., Gebbink, M. F. et al. (2000). Characterization of mouse thrombin-activatable fibrinolysis inhibitor. *Thrombosis & Haemostasis, 83,* 297-303.

Matsuo, O., Lijnen, H. R., Ueshima, S., Kojima, S., & Smyth, S. S. (2007). A guide to murine fibrinolytic factor structure, function, assays, and genetic alterations. *Journal of Thrombosis & Haemostasis, 5,* 680-689.

Miles, L. A., Castellino, F. J., & Gong, Y. (2003). Critical role for conversion of glu-plasminogen to Lys-plasminogen for optimal stimulation of plasminogen activation on cell surfaces. *Trends in Cardiovascular Medicine, 13,* 21-30.

Moghadasian, M. H., McManus, B. M., Nguyen, L. B., Shefer, S., Nadji, M., Godin, D. V. et al. (2001). Pathophysiology of apolipoprotein E deficiency in mice: relevance to apo E-related disorders in humans. *FASEB Journal, 15,* 2623-2630.

Mosnier, L. O., Buijtenhuijs, P., Marx, P. F., Meijers, J. C., & Bouma, B. N. (2003). Identification of thrombin activatable fibrinolysis inhibitor (TAFI) in human platelets. *Blood, 101,* 4844-4846.

Myles, T., Nishimura, T., Yun, T. H., Nagashima, M., Morser, J., Patterson, A. J. et al. (2003b). Thrombin activatable fibrinolysis inhibitor, a potential regulator of vascular inflammation. *Journal of Biological Chemistry, 278,* 51059-51067.

Myles, T., Nishimura, T., Yun, T. H., Nagashima, M., Morser, J., Patterson, A. J. et al. (2003a). Thrombin activatable fibrinolysis inhibitor, a potential regulator of vascular inflammation. *Journal of Biological Chemistry, 278,* 51059-51067.

Nakashima, Y., Plump, A. S., Raines, E. W., Breslow, J. L., & Ross, R. (1994). ApoE-deficient mice develop lesions of all phases of atherosclerosis throughout the arterial tree. *Arteriosclerosis and Thrombosis, 14,* 133-140.

Ni, R., Peleg, T., & Gross, P. L. (2012). Atorvastatin delays murine platelet activation in vivo even in the absence of endothelial NO synthase. *Arterioscler.Thromb.Vasc.Biol., 32,* 2609-2615.

Okafor, O. N. & Gorog, D. A. (2015). Endogenous Fibrinolysis: An Important Mediator of Thrombus Formation and Cardiovascular Risk. *Journal of the American College of Cardiology, 65,* 1683-1699.

Ouweneel, A. B., Heestermans, M., Verwilligen, R. A. F., Gijbels, M. J. J., Reitsma, P. H., Van Eck, M. et al. (2017). Silencing of Anticoagulant Protein C Evokes Low-Incident but Spontaneous Atherothrombosis in Apolipoprotein E-Deficient Mice-Brief Report. *Arterioscler.Thromb.Vasc.Biol., 37,* 782-785.

Plug, T. & Meijers, J. C. (2016). Structure-function relationships in thrombin-activatable fibrinolysis inhibitor. *Journal of Thrombosis & Haemostasis, 14,* 633-644.

Plump, A. S. & Breslow, J. L. (1995). Apolipoprotein E and the apolipoprotein E-deficient mouse. *Annu.Rev.Nutr., 15,* 495-518.

Ranby, M. (1982). Studies on the kinetics of plasminogen activation by tissue plasminogen activator. *Biochimica et Biophysica Acta, 704,* 461-469.

Ridker, P. M., Rifai, N., Stampfer, M. J., & Hennekens, C. H. (2000). Plasma concentration of interleukin-6 and the risk of future myocardial infarction among apparently healthy men. *Circulation, 101,* 1767-1772.

Ryan, C. A., Hass, G. M., & Kuhn, R. W. (1974). Purification and properties of a carboxypeptidase inhibitor from potatoes. *Journal of Biological Chemistry, 249,* 5495-5499.

Santamaria, A., Martinez-Rubio, A., Borrell, M., Mateo, J., Ortin, R., & Fontcuberta, J. (2004). Risk of acute coronary artery disease associated with functional thrombin activatable fibrinolysis inhibitor plasma level. *Haematologica, 89,* 880-881.

Schadinger, S. L., Lin, J. H., Garand, M., & Boffa, M. B. (2010). Secretion and antifibrinolytic function of thrombin-activatable fibrinolysis inhibitor from human platelets. *Journal of Thrombosis & Haemostasis, 8,* 2523-2529.

Schneider, C. P., Schwacha, M. G., & Chaudry, I. H. (2004). The role of interleukin-10 in the regulation of the systemic inflammatory response following trauma-hemorrhage. *Biochimica et Biophysica Acta, 1689,* 22-32.

Schneider, M., Boffa, M., Stewart, R., Rahman, M., Koschinsky, M., & Nesheim, M. (2002). Two naturally occurring variants of TAFI (Thr-325 and Ile-325) differ substantially with respect to thermal stability and antifibrinolytic activity of the enzyme. *Journal of Biological Chemistry, 277,* 1021-1030.

Schneider, M., Brufatto, N., Neill, E., & Nesheim, M. (2004). Activated thrombin-activatable fibrinolysis inhibitor reduces the ability of high molecular weight fibrin degradation products to protect plasmin from antiplasmin. *Journal of Biological Chemistry, 279,* 13340-13345.

Schneider, M. & Nesheim, M. (2003). Reversible inhibitors of TAFIa can both promote and inhibit fibrinolysis. *Journal of Thrombosis & Haemostasis, 1,* 147-154.

Schneider, M. & Nesheim, M. (2004). A study of the protection of plasmin from antiplasmin inhibition within an intact fibrin clot during the course of clot lysis. *Journal of Biological Chemistry, 279,* 13333-13339.

Shinohara, T., Sakurada, C., Suzuki, T., Takeuchi, O., Campbell, W., Ikeda, S. et al. (1994). Pro-carboxypeptidase R cleaves bradykinin following activation. *Int.Arch.Allergy Immunol., 103,* 400-404.

Soeki, T. & Sata, M. (2016). Inflammatory Biomarkers and Atherosclerosis. *Int.Heart J., 57,* 134-139.

Statistics Canada. (2016a). Leading causes of death by sex (Both sexes).

Statistics Canada. (2016b). Report: Achieving heart health targets would lead to big savings for Canada.

Tabas, I. (2009). Macrophage apoptosis in atherosclerosis: consequences on plaque progression and the role of endoplasmic reticulum stress. *Antioxid.Redox.Signal., 11,* 2333-2339.

Tanaka, T., Narazaki, M., & Kishimoto, T. (2014). IL-6 in inflammation, immunity, and disease. *Cold Spring Harb.Perspect.Biol., 6,* a016295.

Tegos, T. J., Kalodiki, E., Sabetai, M. M., & Nicolaides, A. N. (2001). The genesis of atherosclerosis and risk factors: a review. *Angiology, 52,* 89-98.

Thakore, A. H., Guo, C. Y., Larson, M. G., Corey, D., Wang, T. J., Vasan, R. S. et al. (2007). Association of multiple inflammatory markers with carotid intimal medial thickness and stenosis (from the Framingham Heart Study). *Am.J.Cardiol., 99,* 1598-1602.

Thomas, G. R., Thibodeaux, H., Errett, C. J., Badillo, J. M., Keyt, B. A., Refino, C. J. et al. (1994). A long-half-life and fibrin-specific form of tissue plasminogen activator in rabbit models of embolic stroke and peripheral bleeding. *Stroke, 25,* 2072-2078.

Tregouet, D. A., Schnabel, R., Alessi, M. C., Godefroy, T., Declerck, P. J., Nicaud, V. et al. (2009). Activated thrombin activatable fibrinolysis inhibitor levels are associated with the risk of cardiovascular death in patients with coronary artery disease: the AtheroGene study. *Journal of Thrombosis & Haemostasis, 7,* 49-57.

Trigatti, B. L. & Fuller, M. (2016). HDL signaling and protection against coronary artery atherosclerosis in mice. *J.Biomed.Res., 30,* 94-100.

Van Herck, J. L., De Meyer, G. R., Martinet, W., Van Hove, C. E., Foubert, K., Theunis, M. H. et al. (2009). Impaired fibrillin-1 function promotes features of plaque instability in apolipoprotein E-deficient mice. *Circulation, 120,* 2478-2487.

van Tilburg, N. H., Rosendaal, F. R., & Bertina, R. M. (2000). Thrombin activatable fibrinolysis inhibitor and the risk for deep vein thrombosis. *Blood, 95,* 2855-2859.

Van Vre, E. A., Ait-Oufella, H., Tedgui, A., & Mallat, Z. (2012). Apoptotic cell death and efferocytosis in atherosclerosis. *Arterioscler.Thromb.Vasc.Biol., 32,* 887-893.

Vanhoof, G., Wauters, J., Schatteman, K., Hendriks, D., Goossens, F., Bossuyt, P. et al. (1996). The gene for human carboxypeptidase U (CPU)--a proposed novel regulator of plasminogen activation--maps to 13q14.11. *Genomics, 38,* 454-455.

Verhoye, E. & Langlois, M. R. (2009). Circulating oxidized low-density lipoprotein: a biomarker of atherosclerosis and cardiovascular risk? *Clin.Chem.Lab Med., 47,* 128-137.

Walker, J. B. & Nesheim, M. E. (2001). A kinetic analysis of the tissue plasminogen activator and DSPAalpha1 cofactor activities of untreated and TAFIa-treated soluble fibrin degradation products of varying size. *Journal of Biological Chemistry, 276,* 3138-3148.

Wang, X., Smith, P. L., Hsu, M. Y., Ogletree, M. L., & Schumacher, W. A. (2006). Murine model of ferric chloride-induced vena cava thrombosis: evidence for effect of potato carboxypeptidase inhibitor. *Journal of Thrombosis & Haemostasis, 4,* 403-410.

Weisel, J. W. (2005). Fibrinogen and fibrin. *Adv.Protein Chem., 70,* 247-299.

Welch, C. L., Sun, Y., Arey, B. J., Lemaitre, V., Sharma, N., Ishibashi, M. et al. (2007). Spontaneous atherothrombosis and medial degradation in Apoe-/-, Npc1-/- mice. *Circulation, 116,* 2444-2452.

Willemse, J. L., Heylen, E., Nesheim, M. E., & Hendriks, D. F. (2009). Carboxypeptidase U (TAFIa): a new drug target for fibrinolytic therapy? *Journal of Thrombosis & Haemostasis, 7,* 1962-1971.

Xiao, Q., Danton, M. J., Witte, D. P., Kowala, M. C., Valentine, M. T., Bugge, T. H. et al. (1997). Plasminogen deficiency accelerates vessel wall disease in mice predisposed to atherosclerosis. *Proc.Natl.Acad.Sci.U.S.A, 94,* 10335-10340.

Xiao, Q., Danton, M. J., Witte, D. P., Kowala, M. C., Valentine, M. T., & Degen, J. L. (1998). Fibrinogen deficiency is compatible with the development of atherosclerosis in mice. *J.Clin.Invest, 101,* 1184-1194.

Yasar, Y. S., Kuru, P., Toksoy, O. E., & Agirbasli, M. (2014). Functional stability of plasminogen activator inhibitor-1. *ScientificWorldJournal., 2014,* 858293.

Ye, J., Esmon, N. L., Esmon, C. T., & Johnson, A. E. (1991). The active site of thrombin Is altered upon binding to thrombomodulin two distinct structural changes are detected by fluorescence, but only one correlates with protein C activation. *Journal of Biological Chemistry, 266,* 23016-23021.

Zhang, S. H., Reddick, R. L., Piedrahita, J. A., & Maeda, N. (1992). Spontaneous hypercholesterolemia and arterial lesions in mice lacking apolipoprotein E. *Science, 258,* 468-471.

Zhou, J., Kochan, J., Yin, O., Warren, V., Zamora, C., Atiee, G. et al. (2017). A first-in-human study of DS-1040, an inhibitor of the activated form of thrombin-activatable fibrinolysis inhibitor, in healthy subjects. *Journal of Thrombosis & Haemostasis, 15,* 961-971.

Zhou, X., Fragala, M. S., McElhaney, J. E., & Kuchel, G. A. (2010). Conceptual and methodological issues relevant to cytokine and inflammatory marker measurements in clinical research. *Curr.Opin.Clin.Nutr.Metab Care, 13,* 541-547.

Zorio, E., Castello, R., Falco, C., Espana, F., Osa, A., Almenar, L. et al. (2003). Thrombin-activatable fibrinolysis inhibitor in young patients with myocardial infarction and its relationship with the fibrinolytic function and the protein C system. *British Journal of Haematology, 122,* 958-965.